

Manuscript Number: WR38815R1

Title: Photodegradation and ecotoxicology of acyclovir in water under UV254 and UV254/H2O2 processes

Article Type: Research Paper

Keywords: UVC, hydrogen peroxide photolysis, microreactor, ecotoxicity, water reuse, acyclovir removal.

Corresponding Author: Professor Raffaele Marotta, Ph.D

Corresponding Author's Institution: University

First Author: Raffaele Marotta, Ph.D

Order of Authors: Raffaele Marotta, Ph.D; Danilo Russo; Antonietta Siciliano; Marco Guida; Emilia Galdiero; Angela Amoresano; Roberto Andreozzi; Nuno M Reis; Gianluca Li Puma

Abstract: The photochemical and ecotoxicological fate of acyclovir (ACY) through UV254 direct photolysis and in the presence of hydroxyl radicals (UV254/H2O2 process) were investigated in a microcapillary film (MCF) array photoreactor, which provided ultrarapid and accurate photochemical reaction kinetics. The UVC phototransformation of ACY was found to be unaffected by pH in the range from 4.5 to 8.0 and resembled an apparent autocatalytic reaction. The proposed mechanism included the formation of a photochemical intermediate ( $[^1\text{ACY}] = (1.62 \pm 0.07) \times 10^{-3} \text{ mol} \cdot \text{L}^{-1}$ ) that further reacted with ACY to form by-products ( $k' = (5.64 \pm 0.03) \times 10^{-3} \text{ M}^{-1} \cdot \text{s}^{-1}$ ). The photolysis of ACY in the presence of hydrogen peroxide accelerated the removal of ACY as a result of formation of hydroxyl radicals. The kinetic constant for the reaction of OH radicals with ACY ( $k_{\text{OH/ACY}} = (1.23 \pm 0.07) \times 10^9 \text{ M}^{-1} \cdot \text{s}^{-1}$ ) determined with the kinetic modeling method was  $(1.23 \pm 0.07) \times 10^9 \text{ M}^{-1} \cdot \text{s}^{-1}$  and with the competition kinetics method was  $(2.30 \pm 0.11) \times 10^9 \text{ M}^{-1} \cdot \text{s}^{-1}$  with competition kinetics. The acute and chronic effects of the treated aqueous mixtures on different living organisms (*Vibrio fischeri*, *Raphidocelis subcapitata*, *D. magna*) revealed significantly lower toxicity for the samples treated with UV254/H2O2 in comparison to those collected during UV254 treatment. This result suggests that the addition of moderate quantity of hydrogen peroxide (30–150  $\text{mg} \cdot \text{L}^{-1}$ ) might be a useful strategy to reduce the ecotoxicity of UV254 based sanitary engineered systems for water reclamation.

Dear Editor,

please find enclosed a copy of the paper “*Photodegradation and ecotoxicology of acyclovir in water under UV<sub>254</sub> and UV<sub>254</sub>/H<sub>2</sub>O<sub>2</sub> processes*” by Danilo Russo, Antonietta Siciliano, Marco Guida, Emilia Galdiero, Angela Amoresano, Roberto Andreozzi, Nuno M. Reis, Gianluca Li Puma and Raffaele Marotta, which has been revised according to the Referees’ suggestions (all the corrections and new insertions have been printed in **red bold** typefaces).

We thank the Reviewers for the valuable suggestions that helped us to ameliorate the text. Thank you again for your assistance and cooperation.

Napoli, 3/6/2017

Yours sincerely

The Authors

**Reviewer #1:** The study targets at evaluating the UV and UV/H<sub>2</sub>O<sub>2</sub> treatment processes of the antiviral drug acyclovir. A microcapillary film array photoreactor was used to perform part of the experiments to reduce total volumes and time. At the same time 3 well-known bioassays were used to assess the effects of treated acyclovir solutions.

The manuscript is well written. The manuscript should be improved as follows.

**Criticism.** It is not clear how UV is a better treatment process than chlorination to overcome antibiotic resistant bacteria. The strengths and restrictions of the proposed treatment process should be clearly presented to better appreciate the study's findings.

**Response:** *We thank the reviewer for the comment. We added some statements in the introduction to clarify this aspect*

**Criticism.** A thorough literature review of research related to acyclovir, with the current state of the art as well as gaps-of-knowledge is currently missing from the introduction. Many studies have been done using acyclovir and UV<sub>254</sub> treatment.

**Response:** *At the best of our knowledge, as stated in the introduction, no investigations have been reported on the photochemical transformation of ACY under UV<sub>254</sub> and UV<sub>254</sub>/H<sub>2</sub>O<sub>2</sub> treatments and on the ecotoxicological assessments on highly diluted treated solutions containing ACY. On the contrary, photodegradation pathways of ACY under artificial and natural solar light irradiation have been recently investigated (Zhou et al., Photolysis of three antiviral drugs acyclovir, zidovudine and lamivudine in surface freshwater and seawater. Chemosphere 138 (2015) 792–797; Prasse et al., Co-occurrence of photochemical and microbiological transformation processes in open-water unit process wetlands. Environmental Science & Technology 49 (2015) 14136–14145).*

**Criticism.** The rationale for using the specific bioassays, except their wide use and acceptance should be justified.

**Response:** *The rationale for using these bioassays is the key information that need to be collected to determine the efficiency of the system investigated. In particular, in order to identify adverse human health and to take into account the ecotoxicity of the treated samples, we decided to use not only bacteria and microcrustacean but also algae and chronic test with Daphnia magna. These data are important because the continuous release of pharmaceuticals in the aquatic environment also at low concentrations and the importance of sublethal effects in the biota should be considered.*

**Criticism.** The analytical procedure should be described with greater detail. In some assays more toxic byproducts were observed. An attempt should be made to identify the toxic byproducts in order to increase the study's outcomes.

**Response:** *As reported in several sections of the manuscript (abstract, introduction and conclusions), the present paper is a first investigation on the UV<sub>254</sub>/H<sub>2</sub>O<sub>2</sub> photodegradation kinetics of ACY in distilled water and on the ecotoxicity of highly diluted treated samples. The analytical analysis of the phototransformation products, which differ among them depending to presence or absence of hydrogen peroxide and the UV-dose adopted, is very complex and requires (i) an accurate investigation about the fragmentation of acyclovir and the intermediates formed during UV<sub>254</sub> and UV<sub>254</sub>/H<sub>2</sub>O<sub>2</sub> processes using different diagnostic techniques (HPLC-MS/MS, GC-MS and NMR); (ii) a separation of the main photoproducts in order to check their ecotoxicity. The results collected from a large experimental campaign, which requires several months of experimental work, would be reasonably discussed in another extended dedicated analytical paper. However, a very preliminary analysis on sample submitted to UV<sub>254</sub> and UV<sub>254</sub>/H<sub>2</sub>O<sub>2</sub> processes indicated, as main photo-transformation by-products the presence of hydroxylated ACY based intermediates in the UV<sub>254</sub> treatment process, and hydroxylated imidazole based compounds or species formed by the fragmentation of the pyrimidine ring in the UV<sub>254</sub>/H<sub>2</sub>O<sub>2</sub> treatment process. The results have been inserted in the manuscript in order to support the different trends of ecotoxicity observed on the samples submitted to two photolytic processes.*

*It is obvious that major efforts will be necessary to better characterize the mixtures treated at different UV<sub>254</sub> doses.*

**Criticism.** It is not clear how the results from the microcapillary reactor and the photoreactor are comparable. The advantages of the microcapillary reactor should be enhanced so that the reader can understand why both type of experiments were needed.

**Response:** *A key benefit of the microcapillary flow photoreactor over the batch annular photoreactor is the possibility to carry out the process using very small quantities of reagents in a highly controlled environment (the statement has been introduced in the revised text). Consequently, as stated in the original version of the manuscript, the adoption of microphotoreactor technology is particularly appropriate for investigations on such highly priced or scarcely available commercial substances, including illicit drugs or selected pharmaceuticals. On the contrary, as discussed in section 3.2, a cylindrical batch photoreactor (0.480 L) was used to provide sufficient sample volumes to carry out the ecotoxicity tests and the chemical intermediates analysis at varying treatment times.*

**Criticism.** The experiments should be also performed using real or simulated environmental matrices in order to increase their environmental relevance.

**Response:** *The kinetics of photodegradation of an organic substrate in real matrices (urban wastewater effluent, surface water, etc) are highly influenced by their composition (i.e. nature and concentration of the inorganic and organic species, pH, etc..). These variables change depending on the nature of the influent and the type of the physico-chemical treatment adopted. In the present paper we investigated the kinetics of acyclovir under UV<sub>254</sub> irradiation in distilled water.*

*For toxicity tests, neither real nor other simulated environmental matrices were used, considering the large number of chemicals in an effluent and the possibility of interactions (e.g. synergy or additivity) between them and the byproducts of treated solutions.*

*Moreover, as stated in the conclusions of the manuscript (original version), further efforts are required to evaluate possible cumulative effects of the different species occurring in STP effluents. For this reason, these effects cannot be evaluated and consequently generalized using a single real matrix. However, some additional runs performed in synthetic wastewater were carried out and the results inserted in the text (figures 2l-m) in order to validate the kinetic model proposed.*

**Criticism.** It is not clear what was the initial concentration of acyclovir when the microcapillary experiments were performed.

**Response:** *Required information was added in section 3.1. of the manuscript.*

**Criticism.** No explanation on the statistical analysis of results are presented. For instance the LOD/LOQ, the deviation, the QC/QA are not described in detail.

**Response:** *The required control data were reported in the text and referred to the pertinent paragraphs.*

**Criticism.** The discussion section could be augmented in context and length to increment the study's findings.

**Response:** *Following the reviewer's suggestion, we added additional information about the mineralization degree, the photodegradation of ACY in synthetic effluents and the proposed structures of main by-products.*

**Criticism.** The methods for evaluating the biochemical endpoints could be described in greater detail. Apart from this, reference on the method used should be given.

**Response:** *Additional information have been added as suggested by the reviewer.*

**Reviewer #2:** The manuscript WR38815 presents an interesting research work related to the photodegradation and ecotoxicology of acyclovir in water under  $UV_{254}$  and  $UV_{254}/H_2O_2$  processes. The information gathered in this work is relevant for the scientific community, therefore, the manuscript can be accepted for WR after minor revisions.

**Criticism.** The standard errors of the kinetic constants must have only one significant number (example:  $1.62 \pm 0.07$ ;  $5.64 \pm 0.03$ ;  $2.3 \pm 0.1$ ;  $1.23 \pm 0.07$ ).

**Response:** *Done*

**Criticism.** Please define all the variables used in the kinetic models and include units.

**Response:** *The photon fluxes per unit volume emitted by the UV lamp ( $P_o$ ) and the MCF average optical path length ( $l_{MCF}$ ) have been defined in section 3.1 of the original version of the manuscript (lines 132-136). The term  $\epsilon_{254}^{ACY}$ , as reported in the manuscript (original version, lines 253-254), is the molar absorption coefficient at 254 nm for ACY at pH 4.5, 6.0 and 8.0 ( $1.21 \cdot 10^{-2} M^{-1} \cdot cm^{-1}$ ), whereas  $\phi_{ACY}$  and  $k'$  are the quantum yield of photolysis of ACY at 254 nm (lines 248-249) and the kinetic constant for reaction in scheme 1 (lines 249). The respective values and units are reported at lines 260-261 (original version).*

*Additional information has been added in the revised version of the paper (caption for table 2).*

**Criticism.** Please include the kinetics of acyclovir degradation in a real matrix (urban wastewater after secondary treatment).

**Response:** *We thank the reviewer for the suggestion, however, on the basis of our experience, the kinetics of the direct and indirect photodegradation of an organic substrate in real matrices (urban wastewater effluent, surface water, etc) are strongly affected by the nature and the concentration of the inorganic and organic substances contained. These variables change depending on the nature of the influent and the type of the physico-chemical treatment adopted. The present paper is a first preliminary investigation on the kinetics of acyclovir under  $UV_{254}$  irradiation in distilled water. Moreover, as stated in the conclusions of the manuscript (original version), further efforts are required to evaluate possible cumulative effects of the different species occurring in STP effluents. For these reasons, these effects cannot be evaluated and consequently generalized using a single real matrix.*

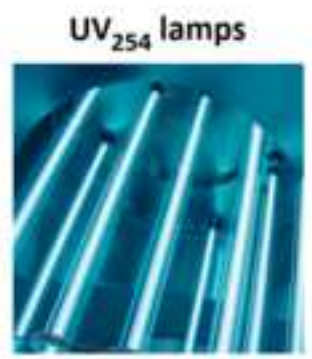
**Criticism.** Please include some information about the mineralization of acyclovir and degradation by-products.

**Response:** *The analytical analysis of the phototransformation products, which differ among them depending to presence or absence of hydrogen peroxide and the UV-dose adopted, is very complex and it requires (i) an accurate investigation about the fragmentation of acyclovir and the intermediates formed during UV<sub>254</sub> and UV<sub>254</sub>/H<sub>2</sub>O<sub>2</sub> processes using different diagnostic techniques (HPLC-MS/MS, GC-MS and NMR); (ii) a separation of the main photoproducts in order to check their ecotoxicity. The results collected from a large experimental campaign, which requires several months of experimental work, would be reasonably discussed in another extended dedicated analytical paper. However, a very preliminary analysis on treated samples (reported in the revised version of the manuscript) indicated, as main photo-transformation by-products, the presence of hydroxylated ACY based intermediates in the UV<sub>254</sub> treatment process, and hydroxylated imidazole based compounds or species formed by the fragmentation of the pyrimidine ring in the UV<sub>254</sub>/H<sub>2</sub>O<sub>2</sub> treatment process. Moreover, TOC removal degrees were inserted in table 3 and in the revised text.*

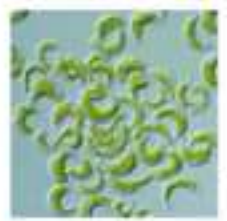
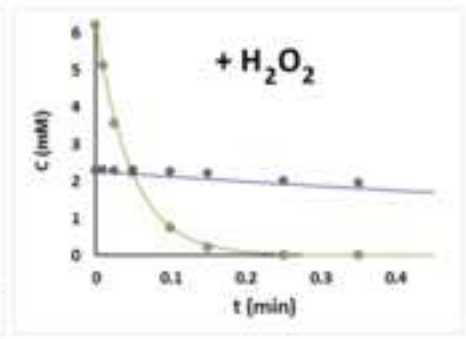
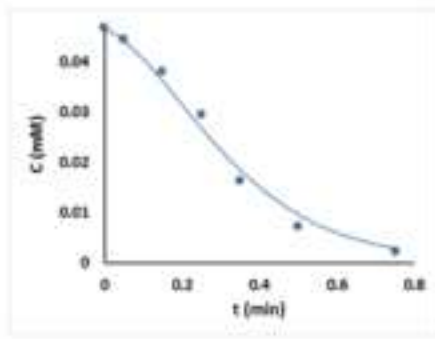
## \*Highlights (for review)

- Photolysis and UV/H<sub>2</sub>O<sub>2</sub> degradation of acyclovir were studied in a microphotoreactor
- UV<sub>254</sub> photolysis quantum yield of acyclovir was estimated ( $1.62 \cdot 10^{-3} \text{ mol} \cdot \text{ein}^{-1}$ )
- Kinetic constant of hydroxyl radical attack to acyclovir was evaluated
- H<sub>2</sub>O<sub>2</sub> assisted photo-oxidation process reduces the ecotoxicity of acyclovir





**Kinetics**



**Ecotoxicity**

1 **Photodegradation and ecotoxicology of acyclovir in water under UV<sub>254</sub> and**  
2 **UV<sub>254</sub>/H<sub>2</sub>O<sub>2</sub> processes**

3

4 Danilo Russo<sup>a</sup>, Antonietta Siciliano<sup>b</sup>, Marco Guida<sup>b</sup>, Emilia Galdiero<sup>b</sup>, Angela Amoresano<sup>c</sup>,  
5 Roberto Andreozzi<sup>a</sup>, Nuno M. Reis<sup>d,e</sup>, Gianluca Li Puma<sup>e,‡</sup> and Raffaele Marotta<sup>a,†</sup>

6

7 <sup>a</sup> Dipartimento di Ingegneria Chimica, dei Materiali e della Produzione Industriale, Università di  
8 Napoli Federico II, p.le V. Tecchio 80, Napoli, Italy.

9 <sup>b</sup> Dipartimento di Biologia, Università di Napoli Federico II, Complesso Universitario Monte  
10 Sant'Angelo, via Cinthia 4, Napoli, Italy.

11 <sup>c</sup> Dipartimento di Scienze Chimiche, Università di Napoli Federico II, Complesso Universitario  
12 Monte Sant'Angelo, via Cinthia 4, Napoli, Italy.

13 <sup>d</sup> Department of Chemical Engineering, University of Bath, Claverton Down, Bath BA2 7AY, UK.

14 <sup>e</sup> Environmental Nanocatalysis & Photoreaction Engineering Department of Chemical Engineering,  
15 Loughborough University, Loughborough LE11 3TU, UK.

16

17 <sup>†</sup> *Corresponding author:* Tel.: +39(0)817682968, fax: +39815936936. E-mail address:  
18 rmarotta@unina.it (R. Marotta).

19 <sup>‡</sup> *Corresponding author:* Tel.: +44(0)1509222510, fax: +44(0)1509223923. E-mail address:  
20 G.Lipuma@lboro.ac.uk (G. Li Puma).

21

22 **Abstract**

23 The photochemical and ecotoxicological fate of acyclovir (ACY) through UV<sub>254</sub> direct photolysis  
24 and in the presence of hydroxyl radicals (UV<sub>254</sub>/H<sub>2</sub>O<sub>2</sub> process) were investigated in a microcapillary  
25 film (MCF) array photoreactor, which provided ultrarapid and accurate photochemical reaction

26 kinetics. The UVC phototransformation of ACY was found to be unaffected by pH in the range  
27 from 4.5 to 8.0 and resembled an apparent autocatalytic reaction. The proposed mechanism  
28 included the formation of a photochemical intermediate ( $\phi_{ACY} = (1.62 \pm 0.07) \cdot 10^{-3} \text{ mol-ein}^{-1}$ ) that  
29 further reacted with ACY to form by-products ( $k' = (5.64 \pm 0.03) \cdot 10^{-3} \text{ M}^{-1} \cdot \text{s}^{-1}$ ). The photolysis of  
30 ACY in the presence of hydrogen peroxide accelerated the removal of ACY as a result of formation  
31 of hydroxyl radicals. The kinetic constant for the reaction of OH radicals with ACY ( $k_{OH/ACY}$ )  
32 determined **with the kinetic modeling method was**  $(1.23 \pm 0.07) \cdot 10^9 \text{ M}^{-1} \cdot \text{s}^{-1}$  **and with the**  
33 **competition kinetics method was**  $(2.30 \pm 0.11) \cdot 10^9 \text{ M}^{-1} \cdot \text{s}^{-1}$  with competition kinetics. The acute  
34 and chronic effects of the treated aqueous mixtures on different living organisms (*Vibrio fischeri*,  
35 *Raphidocelis subcapitata*, *D. magna*) revealed significantly lower toxicity for the samples treated  
36 with UV<sub>254</sub>/H<sub>2</sub>O<sub>2</sub> in comparison to those collected during UV<sub>254</sub> treatment. This result suggests that  
37 the addition of moderate quantity of hydrogen peroxide (30-150 mg·L<sup>-1</sup>) might be a useful strategy  
38 to reduce the ecotoxicity of UV<sub>254</sub> based sanitary engineered systems for water reclamation.

39  
40 *Keywords:* UVC, hydrogen peroxide photolysis, microreactor, ecotoxicity, water reuse, acyclovir  
41 removal.

## 43 **1. Introduction**

44 Water reclamation and water reuse is becoming increasingly common in industrialized countries  
45 with high water demands and in water stressed regions characterized by considerable scarcity of  
46 freshwater (Hoekstra, 2014). The most common treatment method for water reuse is chlorination at  
47 typical dosages ranging from 5 to 20 mg/L with a maximum of two hours of contact time (Asano,  
48 1998). However, concerns related to (i) the adverse impacts of chlorine on irrigated crops, (ii) the  
49 high ecotoxicity of chlorinated by-products (DBPs) formed during the chlorination stage  
50 (Richardson et al., 2007) **and** (iii) the survival of antibiotics resistant bacteria during chlorination

51 (Khan et al., 2016) **with a possible selection of some antibiotic resistance genes in the**  
52 **wastewater microbial community (Huang et al., 2011)** should drive the **transition** from chlorine  
53 disinfection to other more ecofriendly suitable methods. UV radiation treatment (especially UVC,  
54  $\lambda < 280$  nm) produces a high sterilization efficiency (Montemayor et al., 2008) and **could represent**  
55 a viable alternative to chlorination for the disinfection and reuse of effluents from wastewater  
56 treatment plant (WWTP) for irrigation (i.e., after membrane filtration and/or reverse osmosis) **or**  
57 **for aquifer recharge**. Numerous wastewater sites have adopted UVC treatment for effluents  
58 disinfection. For example, Florida and California have favored wastewater reuse and adopted  
59 specific regulations on reclamation technologies through UV disinfection processes. UVC doses  
60 (fluence) ranging from  $50 \text{ mJ}\cdot\text{cm}^{-2}$  to  $150 \text{ mJ}\cdot\text{cm}^{-2}$  have been suggested to efficiently inactivate  
61 pathogens accounting for the variability in the effluent composition (NWRI, 2012), **although**  
62 German and Austrian regulations (DVGW,1997; ONorm, 2001) **suggest the use** of  $40 \text{ mJ}\cdot\text{cm}^{-2}$   
63 **UVC fluence** to eliminate a large variety of bacteria and viruses (**Conner-Kerr et al., 1998**). **Even**  
64 **though UV disinfection has been reported highly effective in the reduction of antibiotic**  
65 **resistance bacteria (ARB), particularly in comparison to chlorination (Shi et al., 2013; Hijnen**  
66 **et al., 2006), other investigations have demonstrated that UV disinfection may not contribute**  
67 **to the significant reduction of selected ARB, such as tetracycline-and sulfonamide-resistant**  
68 **bacteria (Munir et al., 2011; Meckes, 1982) thus indicating a plausible selectivity of UV on**  
69 **ARB (Guo et al., 2013).**  
70 **Moreover**, numerous studies have suggested that under the **recommended** UVC doses several  
71 biorefractory xenobiotics, **particularly** pharmaceuticals and personal care products generally  
72 occurring in municipal discharges and partially removed in WWTPs, may undergo photochemical  
73 transformations induced by UVC irradiation (Canonica et al., 2008; Nick et al., 1992; Pereira et al,  
74 2007; Kim et al., 2009; Ma et al., 2016; Kovacic et al., 2016; Liu et al., 2016; Marotta et al., 2013)  
75 which may generate by-products with high ecotoxicity (Rozas et al., 2016; Yuan et al., 2011). For  
76 these reasons, the use of hydrogen peroxide during UVC disinfection (**UV<sub>254</sub>/H<sub>2</sub>O<sub>2</sub>**) **which**

77 **produces highly reactive radical species**, has been proposed as a viable **treatment for effective**  
78 removal of micropollutant **and ARB** and, in consequence, **for the reduction of** the ecotoxicity risk  
79 (García-Galan et al., 2016; Melo da Silva et al., 2016).

80 Among the emerging Pharmaceuticals and Personal Care Products detected in WWTP effluents,  
81 antiviral drugs play a leading role (Richardson, 2012; Jain et al., 2013) **due to their** scarce  
82 biodegradability (Funke et al., 2016) and increased usage during the last decade, **particularly** for  
83 the treatment of viral diseases and for the prevention of pandemic outbreaks (Hill et al., 2014).  
84 Moreover, antiviral drugs have been considered as **some** of the most hazardous therapeutic  
85 substances **exerting** high toxicity towards biota, such as crustaceans, fish and algae (Sanderson et  
86 al., 2004). The presence of antiviral drugs in the environment **raises** considerable concern  
87 **regarding their** potential effect on the ecosystem, **with the potential of developing** antiviral drug  
88 resistance, in analogy to **the development of** antibiotic resistant bacteria (Singer et al., 2007;  
89 Gillman et al., 2015).

90 Acyclovir (ACY) is one of the oldest and most widely used antiviral drug for treating two common  
91 viral infections (chickenpox-zoster and herpes simplex) and it is also prescribed to patients with  
92 weakened immune systems in order to control viral infections (i.e., viral conjunctivitis) (Bryan-  
93 Marrugo et al., 2015). ACY has been recently detected in different WWTP effluents as well as in  
94 surface water at level of few nanograms per liter up to over one micrograms per liter (Table 1).

95 **The** photodegradation pathways of ACY under artificial and natural solar light irradiation have  
96 been recently investigated (Zhou et al., 2015; Prasse et al., 2015). However, **there is a lack of**  
97 investigations on the photochemical transformation of ACY under UV<sub>254</sub> and UV<sub>254</sub>/H<sub>2</sub>O<sub>2</sub>  
98 treatments and on the **simultaneous** ecotoxicological assessments **of** highly diluted treated solutions  
99 containing ACY.

100 More information is needed to determine **the effectiveness** of UV<sub>254</sub> assisted processes **on the**  
101 **removal** of ACY **from** aqueous solutions **and the impact that these processes may have on the**  
102 **structure of aquatic communities and on the ecosystem dynamics.**

103 **The use of microcapillary flow photoreactors has recently been proposed to intensify the**  
104 **treatment of substances that are either** highly priced, scarcely commercially available or  
105 controlled substances such as illicit drugs or selected pharmaceuticals (Reis and Li Puma, 2015;  
106 Russo et al., 2016). **In contrast to conventional laboratory photochemical systems which**  
107 **require relatively larger volume of liquid,** photochemical treatments in microphotoreactors are  
108 carried out **in a highly controlled environment** with minimal sample volumes (of the order of few  
109 mL), the sufficient amount to generate samples for subsequent analysis. Furthermore,  
110 photochemical transformations in microphotoreactors are executed at extremely short residence  
111 times (of the order of seconds) in comparison to conventional laboratory photoreactors, **resulting in**  
112 **an efficient use of time and resources.**

113 **Under this background, in this study we investigated** the degradation kinetics of ACY in  
114 **distilled water** under UV<sub>254</sub> and UV<sub>254</sub>/H<sub>2</sub>O<sub>2</sub> irradiation by means of a microcapillary film (MCF)  
115 array photoreactor and **we evaluated** the acute and chronic ecotoxicity of highly diluted treated  
116 samples using **a range of** selected organisms, to provide important information regarding the  
117 photolysis of ACY in UV<sub>254</sub> based sanitary engineered systems for water reclamation. **The toxicity**  
118 **was assessed considering a battery of toxicity tests (*Aliivibrio fischeri*, *Raphidocelis***  
119 ***subcapitata*, *Daphnia magna*) and endpoints (bioluminescence, growth inhibition,**  
120 **immobilization, survival, reproduction and biomarker) including three trophic and**  
121 **phylogenetic levels (Lofrano et al., 2016).**

122 **The battery of toxicity tests proposed were sensitive indicators of toxic pollutants, and also**  
123 **determined the great diversity of potential stress-receptor that could result from**  
124 **pharmaceuticals and their byproducts entering the environment (FDA, 1998).**

125

## 126 **2. Materials and methods**

### 127 *2.1. Materials*

128 Hydrogen peroxide (30% v/v), ACY (pharmaceutical secondary standard), methanol ( $\geq 99.9\%$  v/v),  
129 formic acid ( $>99\%$  w/w), benzoic acid ( $\geq 99.5\%$  w/w), orthophosphoric acid (85% w/w in H<sub>2</sub>O),  
130 sodium hydroxide ( $>98\%$  w/w), perchloric acid (70% v/v), catalase from *Micrococcus lysodeikticus*  
131 and reagents for ecotoxicity tests were purchased from Sigma-Aldrich. **An aqueous mixture of**  
132 **peptone (32 ppm), meat extract (22 ppm), urea (6 ppm), K<sub>2</sub>HPO<sub>4</sub> (28 ppm), CaCl<sub>2</sub>·H<sub>2</sub>O (4**  
133 **ppm), NaCl (7 ppm) and Mg<sub>2</sub>SO<sub>4</sub> (0.6 ppm) was used for the preparation of a synthetic**  
134 **wastewater according to the OECD Guidelines (Organisation for Economic Cooperation and**  
135 **development, 1999). The substances were purchased from Sigma-Aldrich and used as**  
136 **received.** Milli-Q water was used as solvent in analytical determinations and experiments.

137

## 138 2.2. Analytical methods

139 The concentration of hydrogen peroxide, ACY, and benzoic acid was measured by HPLC (1100  
140 Agilent) equipped with a Gemini 5u C6-Phenyl 110 (Phenomenex) reverse phase column and a  
141 diode array detector. The mobile phase was a mixture of 93% aqueous orthophosphoric acid (10  
142 mM) and 7% methanol flowing at  $8.0 \cdot 10^{-4}$  L·min<sup>-1</sup>. The pH of the aqueous solutions was adjusted  
143 with NaOH or HClO<sub>4</sub> and measured with an Accumet Basic AB-10 pH-meter. The molar  
144 absorption coefficient of ACY was estimated using a Perkin Elmer UV/VIS spectrometer (mod.  
145 Lambda 35). **Total organic carbon (TOC) was monitored by a TOC analyzer (Shimadzu 5000**  
146 **A). MS analysis was performed by direct injection on Agilent 6230 TOF LC/MS coupled with**  
147 **Agilent HPLC system (1260 Series). The mobile phase was a mixture of methanol (10% v/v)**  
148 **and formic acid (0.1% v/v) aqueous solution at flow rate of 0.4 mL·min<sup>-1</sup> and the injection**  
149 **volume of samples was 20  $\mu$ L. The MS source was an electrospray ionization (ESI) interface**  
150 **in the positive ion mode with capillary voltage of 3500 V, gas temperature at 325 °C, dry gas**  
151 **(N<sub>2</sub>) flow at 8 L·min<sup>-1</sup> and the nebulizer at 35 psi. The MS spectra were acquired in a mass**  
152 **range of 100-3000 m/z with a rate of 1 spectrum/s, time of 1000 ms/spectrum and**  
153 **transient/spectrum of 9905.**

154

### 155 **3. Experimental apparatus and procedures**

#### 156 *3.1. MCF array photoreactor*

157 The degradation kinetics of ACY by UV<sub>254</sub> and UV<sub>254</sub>/H<sub>2</sub>O<sub>2</sub> were investigated in a MCF array  
158 photoreactor described elsewhere (Reis et al., 2015; Russo et al., 2016). Briefly, the photoreactor  
159 (Lamina Dielectrics Ltd) consisted of ten **UV<sub>254</sub> transparent** microcapillaries of fluorinated  
160 polymer characterized by a mean hydraulic diameter of 195 μm. The microcapillaries were coiled  
161 around a UV monochromatic (254 nm) lamp (Germicidal G8T5) in the region with uniform  
162 emission. Experiments were carried out at room temperature (~25 °C) in continuous flow through  
163 the reactor at different space times, using capillaries of different length exposed to the UV lamp  
164 irradiation. The flow rate through the MCF was 6.0·10<sup>-4</sup> L·min<sup>-1</sup>. Aqueous samples were collected  
165 from the MCF outlet, and rapidly analyzed by HPLC. At the end of each experimental run, the pH  
166 of the solutions was unchanged. **The initial concentration of ACY used in the experiments**  
167 **ranged between 2.05·10<sup>-5</sup> mol·L<sup>-1</sup> and 4.67·10<sup>-5</sup> mol·L<sup>-1</sup>.**

168 The lamp irradiance was varied by changing the nominal power from 4.5 W to 8.0 W using a  
169 variable power supply unit. The photon fluxes per unit volume emitted by the UV lamp ( $P_o$ ) for  
170 each power setting, estimated by H<sub>2</sub>O<sub>2</sub> actinometry (Nicole et al, 1990; Goldstein et al., 2007), were  
171 1.92·10<sup>-2</sup> ein·(s·L)<sup>-1</sup> (nominal power 8.0 W) and 1.27·10<sup>-2</sup> ein·(s·L)<sup>-1</sup> (nominal power 4.5 W). The  
172 MCF average optical path length ( $l_{MCF}$ ) was 154 μm. All the runs were carried out in duplicate. The  
173 data collected were used to estimate the kinetic unknown parameters (quantum yield of direct  
174 photolysis at 254 nm of ACY and kinetic constant of hydroxyl radical attack to ACY).

175

#### 176 *3.2. Cylindrical batch photoreactor*

177 A cylindrical batch photoreactor ( $V_b = 0.480$  L), equipped with a low-pressure mercury  
178 monochromatic lamp (Helios Italquartz, HGL10T5L, 17W nominal power emitting at 254 nm), was  
179 used to provide **large** sample volumes **required for the** ecotoxicity tests at varying treatment times



180 (i.e., different UV<sub>254</sub> fluence). The UV<sub>254</sub> dose (mJ·cm<sup>-2</sup>) was calculated as the average photon  
181 fluence rate multiplied by the treatment time. The average photon fluence rate emitted by the UV  
182 lamp at 254 nm was 4.7 mW·cm<sup>-2</sup> (UVC DELTA OHM radiometer). The experimental device was  
183 described elsewhere (Spasiano et al., 2016).

184

### 185 3.3. Ecotoxicity assessment

186 Reconstituted aqueous solution (pH =7.8 ± 0.2), was used as dilution water for cladoceran toxicity  
187 tests: CaCl<sub>2</sub>·2H<sub>2</sub>O (290 mg·L<sup>-1</sup>), MgSO<sub>4</sub>·7H<sub>2</sub>O (120 mg·L<sup>-1</sup>), NaHCO<sub>3</sub> (65 mg·L<sup>-1</sup>), KCl (6  
188 mg·L<sup>-1</sup>). Different salts were used for the preparation of algal test medium: CaCl<sub>2</sub>·2H<sub>2</sub>O (18 mg·L<sup>-1</sup>  
189 <sup>1</sup>), MgSO<sub>4</sub>·7H<sub>2</sub>O (15 mg·L<sup>-1</sup>), NH<sub>4</sub>Cl (15 mg·L<sup>-1</sup>), MgCl<sub>2</sub>·6H<sub>2</sub>O (12 mg·L<sup>-1</sup>), KH<sub>2</sub>PO<sub>4</sub> (1.6 mg·L<sup>-1</sup>),  
190 FeCl<sub>3</sub>·6H<sub>2</sub>O (0.08 mg·L<sup>-1</sup>), Na<sub>2</sub>EDTA·2H<sub>2</sub>O (0.1 mg·L<sup>-1</sup>), H<sub>3</sub>BO<sub>3</sub> (0.185 mg·L<sup>-1</sup>), MnCl<sub>2</sub>·4H<sub>2</sub>O  
191 (0.415 mg·L<sup>-1</sup>), ZnCl<sub>2</sub> (0.003 mg·L<sup>-1</sup>), CoCl<sub>2</sub>·6H<sub>2</sub>O (0.0015 mg·L<sup>-1</sup>), Na<sub>2</sub>MoO<sub>4</sub>·2H<sub>2</sub>O (7.0·10<sup>-3</sup>  
192 mg·L<sup>-1</sup>), CuCl<sub>2</sub>·2H<sub>2</sub>O (1.0·10<sup>-5</sup> mg·L<sup>-1</sup>). Reconstitution solution, osmotic adjusting solution (OAS)  
193 and diluent (NaCl 2%) were the reagents used in *Vibrio fischeri* toxicity test (Strategic diagnostics  
194 Inc. SDI).

195 The enzymatic assays chosen to evaluate oxidative stress were ROS (reactive oxygen species)  
196 content using 2,7- dichlorodihydrofluorescein (H<sub>2</sub>DCFDA) and activities of SOD (superoxide  
197 dismutase), CAT (catalase) and GST (glutathione transferase) that were measured using respective  
198 assay kits according to the manufacturer's instruction's (Sigma Aldrich). All determinations were  
199 quantified spectrophotometrically.

200 *V. fischeri*, *R. subcapitata* and acute *D. magna* assays were conducted with an initial ACY  
201 concentration of 1.2 mg·L<sup>-1</sup> and on its related UV<sub>254</sub> and UV<sub>254</sub>/H<sub>2</sub>O<sub>2</sub> treated solutions. Chronic  
202 toxicity and oxidative stress tests on *Daphnia magna* were performed starting on untreated and  
203 treated solutions diluted by 100 fold, in order to assess any differences at sub lethal concentration  
204 levels. **Negative and positive controls were included in each experiment. The significance of**

205 **differences of toxicity between the treated samples and controls was assessed by the analysis**  
206 **of variance (ANOVA) considering a significance threshold level always set at 5%. For higher**  
207 **variance than 5%, post-hoc tests were carried out with Dunnett's method and Tukey's test.**  
208 **Whenever possible, toxicity was expressed as median effective concentration (EC<sub>50</sub>) with 95%**  
209 **confidence limit values. Otherwise, toxicity was expressed as percentage of effect (PE, %).**

210

### 211 3.3.1. *Organisms maintenance and monitoring*

212 Freeze-dried *Vibrio fischeri* (strain NRRL-B-11177) cells were reconstituted with reagent diluent at  
213 4 °C. *Raphidocelis subcapitata* were cultured in ISO medium (ISO, 2012) at 23 ± 2 °C with  
214 continuous 4500 lux light and aeration (0.2 mm filtered air). *Daphnia magna* were cultured at 20 ±  
215 1 °C, with a 16:8 light/dark photoperiod in ISO water (ISO, 2012).

216 Luminescence *V. fischeri* measurements were performed with Microtox® Model 500 Toxicity  
217 Analyzer from Microbics Corporation (AZUR Environmental) equipped with a 30 well incubated at  
218 15 ± 1 °C and with excitation source at 490 nm wavelength.

219 *R. subcapitata* density was determined by an indirect procedure using a spectrophotometer (Hach  
220 Lange DR5000) and cuvette (5 cm). *D. magna* viability, mobility and growth were observed with a  
221 stereomicroscope (LEICA EZ4-HD).

222

### 223 3.3.2. *Bacteria toxicity test*

224 The inhibitory effect of ACY samples on the light emission of *V. fischeri* (strain NRRL-B-11177)  
225 was evaluated with the 11348-3:2007 ISO method (ISO, 2007). Tests were carried out on an ACY  
226 concentration of 1.2 mg·L<sup>-1</sup> and on its related treated by-products solutions. OAS was added to each  
227 sample to ensure that the final NaCl concentration was above 2.0%. The initial light output from  
228 each cuvette containing reconstituted freeze-dried *V. fischeri* was recorded. The test solutions were  
229 then added and after 30 minutes exposure, the final light output was measured. **Positive control**  
230 **tests for *V. fischeri* were carried out with C<sub>6</sub>H<sub>4</sub>Cl<sub>2</sub>O (EC<sub>50</sub> = 4.1 ± 2.2 mg·L<sup>-1</sup>).**

231

### 232 3.3.3. Algae toxicity test

233 The *R. subcapitata* bioassay was conducted following the guidelines ISO 8692 (ISO, 2012). Three  
234 replicates were included for each sample. The replicates were inoculated with  $10^4$  algal cells·mL<sup>-1</sup>  
235 and incubated for 72 h at  $23 \pm 2$  °C under continuous illumination (irradiance range of 120-60  
236  $\mu\text{ein}\cdot\text{m}^{-2}\cdot\text{s}^{-1}$ ). The algal biomass exposed to the samples was compared with the algal biomass in the  
237 negative control. **Positive control tests for *R. subcapitata* were carried out with  $\text{K}_2\text{Cr}_2\text{O}_7$  ( $\text{EC}_{50}$   
238  $= 1 \pm 0.2 \text{ mg}\cdot\text{L}^{-1}$ ).**

239

### 240 3.3.4. Crustaceans toxicity test

241 Acute toxicity tests with *D. magna* were carried out according to ISO 6341 (ISO, 2013). Newborn  
242 daphnids (<24 h old) were exposed in four replicates for 24 h and 48 h at  $20 \pm 1$  °C. Toxicity was  
243 expressed as percentage of immobilized organisms. **Positive control tests for *D. magna* were  
244 carried out with  $\text{K}_2\text{Cr}_2\text{O}_7$  (48h,  $\text{EC}_{50} = 0.6 \pm 0.1 \text{ mg}\cdot\text{L}^{-1}$ ).**

245 The *D. magna* chronic bioassay was carried out according to the guideline OECD 211 (OECD,  
246 2012). Ten *D. magna* neonates (< 24 h hold) were used and individually placed for each treatment  
247 in beakers containing 50 ml of the test solutions, renewed every two other days. Organisms exposed  
248 for 21 days with ACY solutions were then fed one day with *R. subcapitata* ( $10^7$  cell·mL<sup>-1</sup>).  
249 Survival, reproduction and growth were observed daily, and newborns were discarded from  
250 beakers.

251 The amount of ROS produced in *D. magna* was determined using 2,7-dichlorodihydrofluorescein  
252 ( $\text{H}_2\text{DCFDA}$ , Sigma Aldrich) using the method previously reported (Galdiero et al., 2016). After 48  
253 h of exposure, each exposed and not exposed living daphnids were rinsed with deionized water to  
254 remove any excess pharmaceuticals adhered to their body surface and transferred to a 96-well plate.  
255 A selected volume (200  $\mu\text{L}$ ) of 10 mM  $\text{H}_2\text{DCFDA}$  was added to each well and the plate was then  
256 incubated for 4 h in the dark at 20-25°C. Fluorescence was measured using a fluorescence plate

257 reader with an excitation wavelength of 350 nm and an emission of 600 nm. The increase in  
258 fluorescence intensity yielded the ROS quantity compared to control.

259 Exposed and not exposed daphnids were homogenized in 1 mL sucrose buffer (0.25 M sucrose, 0.1  
260 M Tris-HCl, 1 mM EDTA, pH 7.4) and successively centrifuged at 12.000 g for 15 min at 4°C.

261 Supernatants were collected and used to determinate enzymatic activities. Protein content of the  
262 samples was quantified using the protocol described by Bradford (1976) using bovine serum  
263 albumin as standard.

264 CAT activity was expressed as H<sub>2</sub>O<sub>2</sub> consumed (U·mg<sup>-1</sup> of protein) to convert it to H<sub>2</sub>O and O<sub>2</sub> per  
265 minute, per mg protein at 240 nm (Aebi, 1984).

266 SOD activity was calculated by measuring the decrease in the color development of samples at 440  
267 nm with the reference to the xantine oxidase/cithochrome method (Crapo et al., 1978). **In  
268 particular the superoxide radical, generated from the conversion of xanthine to uric acid and  
269 H<sub>2</sub>O<sub>2</sub> by xanthine oxidase, reacts with the tetrazolium salt WST-1 forming formazan.**

270 One unit of SOD was defined as the amount of enzyme required to produce 50% inhibition in the  
271 reaction system.

272 GST was calculated by measuring the changes in absorbance recorded at 340 nm due to the  
273 conjugation of glutathione to 1-chloro-2,4-dinitrobenzene (Habig et al., 1974).

274 One unit of enzyme was the quantity necessary for the reduction of 1 μmol·L<sup>-1</sup> GSH in 1 min at 37  
275 °C.

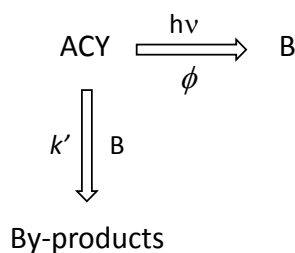
276 **Test runs were performed** in triplicate **with** additional controls **including on** aqueous solutions  
277 containing hydrogen peroxide **supplemented** with catalase, **used** to destroy **the** residual hydrogen  
278 peroxide.

279

## 280 **4. Results and discussion**

### 281 *4.1. UV<sub>254</sub> photolysis: kinetic investigation*

282 The results collected from runs of UV<sub>254</sub> photolysis of ACY in aqueous solution at three different  
 283 pH values (4.5, 6.0 and 8.0) in the MCF photoreactor at varying lamp power are reported in Figs.  
 284 1a-e as a function of the space time. The results indicate that, for a fixed lamp power, the pH did not  
 285 affect the conversion. In fact, for these runs a half-time of about 17 seconds was recorded  
 286 independent of the pH. Moreover, **the analysis** of the concentration vs time profile **demonstrated**  
 287 that the photolysis of ACY resembled an apparent autocatalytic behavior which suggested the  
 288 adoption of an autocatalytic kinetic model to describe the degradation of ACY under the adopted  
 289 experimental conditions. Since the destruction of guanine based substrates under UV<sub>254</sub> irradiation  
 290 has been ascribed to both the direct photolysis of guanine derivatives and the reaction of guanine  
 291 based molecules with the radical species formed during the photolytic process (Crespo-Hernandez  
 292 et al., 2000a,b), the simplified reaction scheme (Scheme 1) was considered for the UV<sub>254</sub> photolysis  
 293 of ACY, which is a guanine derivative:



294

295

Scheme 1

296

297 where B indicates a pseudo intermediate (hydrated electron, oxygen reactive species, etc.) capable  
 298 of reacting with ACY molecules according to a simple autocatalytic-type kinetics. The quantum  
 299 yield of photolysis of ACY at 254 nm ( $\phi_{ACY}$ ) and the kinetic constant  $k'$  were estimated through an  
 300 iterative method, using simultaneously the concentration data reported in Figures 1a,e to solve ODE  
 301 equations 1 and 2:

$$\frac{d[\text{ACY}]}{dt} = -P_o \cdot \phi_{\text{ACY}} \cdot (1 - \exp(-2.3 \cdot l_{\text{MCF}} \cdot \epsilon_{254}^{\text{ACY}} \cdot [\text{ACY}])) - k' \cdot [\text{ACY}] \cdot [\text{B}] \quad (1)$$

$$\frac{d[B]}{dt} = P_o \cdot \phi_{ACY} \cdot (1 - \exp(-2.3 \cdot l_{MCF} \cdot \epsilon_{254}^{ACY} \cdot [ACY])) \quad (2)$$

302 Where  $t$  is the space time in the continuous flow MCF photoreactor (the reaction or exposure time)  
 303 and the term  $\epsilon_{254}^{ACY}$  is the molar absorption coefficient at 254 nm for ACY at pH 4.5, 6.0 and 8.0  
 304 ( $1.21 \cdot 10^{-2} \text{ M}^{-1} \cdot \text{cm}^{-1}$ ). This result is in agreement with the pKa values of ACY (2.27 and 9.25)  
 305 (Florence, 2010).

306 The MATLAB routine “ode45”, based on the Runge-Kutta method with adaptive step-size, was  
 307 used for the optimization procedure which minimized the objective function  $\sum_j^m \sum_i^n (y_{ACY_{j,i}} -$   
 308  $c_{ACY_{j,i}})^2$ , made by the squares of the differences between the calculated “ $y$ ” and experimental “ $c$ ”  
 309 concentrations of ACY, varying the reaction time “ $n$ ” and for different experimental photolytic runs  
 310 “ $m$ ”. The determined kinetic parameters that minimized the objective function were  $\phi_{ACY} = (1.62 \pm$   
 311  $0.07) \cdot 10^{-3} \text{ mol} \cdot \text{ein}^{-1}$  and  $k' = (5.64 \pm 0.03) \cdot 10^{-3} \text{ M}^{-1} \cdot \text{s}^{-1}$ . The comparison between experimental and  
 312 calculated data, reported in Figures 1a-e **including** the percentage standard deviations,  
 313 **demonstrated close prediction of** the concentration profiles of ACY in the MCF photoreactor.

314 The  $\phi_{ACY}$  value reported above has the same order of magnitude **as** the quantum yield of  
 315 photodecomposition of other guanine derivatives, such as guanosine and 9-ethyl-guanine at similar  
 316 concentrations (Crespo-Hernandez et al., 2000a), thus suggesting that the purine structure could  
 317 play a fundamental role in the UV photolysis of guanine derivatives. The differences could be  
 318 ascribed to a slight effect of the nature of the group attached to the 9-N on the UV-photolysis  
 319 kinetics.

320

#### 321 4.2. $UV_{254}/H_2O_2$ oxidation: kinetic investigation

322 The results of a preliminary run carried out in the presence of hydrogen peroxide under darkness  
 323 indicated that ACY was not degraded in the presence of  $H_2O_2$  alone for reaction times up to 30 min.  
 324 Photooxidation experiments of ACY by the  $UV_{254}/H_2O_2$  process were carried out under the same

325 experimental conditions (i.e., pH, lamp power and initial concentration of ACY) used in the UV<sub>254</sub>  
326 direct photolysis runs.

327 The degradation profiles for ACY and H<sub>2</sub>O<sub>2</sub> as a function of space time in the MCF photoreactor  
328 were modeled on the basis of a simplified reaction scheme and the mass balances listed in Table 2.

329 The reaction scheme considers the consumption of ACY and hydrogen peroxide by direct  
330 photolysis (*reactions 3 and 4*). Hydroxyl radicals generated by UV<sub>254</sub> photolysis of H<sub>2</sub>O<sub>2</sub> can react  
331 with hydrogen peroxide (*reaction 5*), ACY (*reaction 6*) and the transformation products (*reaction*  
332 *7*). A radical termination of peroxy radicals was considered in the mechanism (*reaction 8*).

333 The literature reports two different values of the the kinetic constant of the reaction between  
334 hydroxyl radical and ACY ( $k_{OH/ACY}$ ):  $5.0 \cdot 10^9 \text{ M}^{-1} \cdot \text{s}^{-1}$  (pH=9, T=18 °C, solar simulator  $\lambda > 320 \text{ nm}$ )  
335 (Prasse et al., 2015) and  $1.19 \cdot 10^{10} \text{ M}^{-1} \cdot \text{s}^{-1}$  (pH= 6-9, lamp  $\lambda > 340 \text{ nm}$ ) (Zhou et al., 2015) which  
336 were determined with competition kinetics in the presence of a reference compound (i.e.,  
337 acetophenone, Zhou et al., 2015, and p-chloro-benzoic acid, Prasse et al., 2015). Since these  $k_{OH/ACY}$   
338 values **differed** by more than 50%,  $k_{OH/ACY}$  **was determined using both** numerical optimization and  
339 competition kinetics.

340 Specifically, the same iterative optimization procedure reported in section 4.1, using simultaneously  
341 a set of 9 photodegradation runs **in distilled water**, at different initial concentrations of ACY and  
342 hydrogen peroxide, pH and lamp power, was used for the estimation of  $k_{OH/ACY}$ . The iterative  
343 method minimized the objective function (Eq. 14) that in this case was slightly modified to include  
344 the number of the reacting species ( $h$ ):

$$\Phi = \sum_g^h \sum_j^m \sum_i^n (y_{g,j,i} - c_{g,j,i})^2 \quad (14)$$

345 From this method  $k_{OH/ACY}$  was determined as  $(1.23 \pm \mathbf{0.07}) \cdot 10^9 \text{ M}^{-1} \cdot \text{s}^{-1}$ . Graphical examples of the  
346 results obtained by the modeling through the optimization procedure are shown in Figures 2a-f  
347 (*optimization procedure*). In Figures 2g-i the comparison **is reported** between experimental and

348 calculated residual ACY and H<sub>2</sub>O<sub>2</sub> concentration, **when the model was used in simulation mode**  
349 without any further parameter adjustment (*simulation mode*), using the  $k_{OH/ACY}$  kinetic constant  
350 above estimated. It can be noted a good capability of the model of predicting the experimental data  
351 under the adopted conditions.

352 **Two additional UV<sub>254</sub>/H<sub>2</sub>O<sub>2</sub> runs (Figs. 2l-m) were carried out using synthetic wastewater to**  
353 **further validate the kinetic results obtained. The photolytic runs were simulated using the**  
354 **proposed kinetic model properly modified to include the HO radical scavenging effect of the**  
355 **species forming the synthetic matrix (Spasiano et al., 2016). For this purpose, the pseudo-first**  
356 **order rate constant ( $k'_{sca} = 4.01 \cdot 10^9 \text{ s}^{-1}$ ) was considered for the reaction between the hydroxyl**  
357 **radicals and the scavenger species (Spasiano et al., 2016). Also in this case, a good capability of**  
358 **the model was still observed to predict the experimental data under the adopted conditions.**

359 The competition kinetic method was used to estimate the  $k_{OH/ACY}$  constant in the same MCF  
360 photoreactor, to further validate the kinetic model proposed above. The method compares the ACY  
361 concentration decay to that of benzoic acid (BA) (initial concentration  $2.0 \cdot 10^{-5}$  M) chosen as  
362 reference compound (Onstein et al., 1999):

$$\ln\left(\frac{[ACY]}{[ACY]_0}\right) = \frac{k_{OH/ACY}}{k_{OH/BA}} \cdot \ln\left(\frac{[BA]}{[BA]_0}\right) \quad k_{OH/BA} = 5.9 \cdot 10^9 \text{ M}^{-1} \cdot \text{s}^{-1} \quad (\text{pH} = 6.0) \quad (15)$$

363 An average value  $k_{OH/ACY} = (2.30 \pm 0.11) \cdot 10^9 \text{ M}^{-1} \cdot \text{s}^{-1}$  was thus calculated from UV<sub>254</sub>/H<sub>2</sub>O<sub>2</sub>  
364 experiments carried out at pH = 6.0 and  $[H_2O_2]_0/[ACY]_0 = 20$  and **at** different lamp power (4.5 W  
365 and 8.0 W). The difference of this from the value estimated with kinetic modeling may be ascribed  
366 to the intrinsic limitations of the competition kinetics method that does not include the contribution  
367 of ACY consumption by direct photolysis. However, both  $k_{OH/ACY}$  values estimated in the present  
368 investigation were significantly lower than those previously reported in the literature (Zhou et al.,  
369 2015; Prasse et al., 2015).

370  
371 *4.3. UV<sub>254</sub> photolysis and UV<sub>254</sub>/H<sub>2</sub>O<sub>2</sub> oxidation: Ecotoxicity assessment*



372 A battery of ecotoxicity tests on *V. fischeri*, *D. magna* and *R. subcapitata* were **performed** on  
373 untreated and treated aqueous solutions with an initial ACY concentration of  $1.2 \text{ mg}\cdot\text{L}^{-1}$ . The  
374 results showed that the inhibition of *V. fischeri* luminescence remained unchanged in the presence  
375 of the  $\text{UV}_{254}$  and  $\text{UV}_{254}/\text{H}_2\text{O}_2$  irradiated solutions, in comparison to the untreated solution (data not  
376 shown).

377 The results obtained for *D. magna* (exposure time = 24 and 48 h) for the  $\text{UV}_{254}$  and  $\text{UV}_{254}/\text{H}_2\text{O}_2$   
378 treated and untreated samples are reported in Figures 3A,B. The samples treated with  $\text{UV}_{254}$   
379 irradiation in the absence of hydrogen peroxide, initially showed an increase of immobility of  
380 daphnids at increasing  $\text{UV}_{254}$  dose and consequently at higher ACY conversion, suggesting an  
381 increase in acute ecotoxicity, although, this eventually decreased significantly at the highest  $\text{UV}_{254}$   
382 dose. On the other hand, the acute ecotoxicity of the  $\text{UV}_{254}/\text{H}_2\text{O}_2$  treated solutions toward *D. magna*  
383 was significantly lower in comparison to the samples treated with  $\text{UV}_{254}$  only, even at much lower  
384 UV doses. It is important to note that the acute ecotoxicity of the  $\text{UV}_{254}$  sample after complete  
385 conversion of ACY was higher than the value for the un-irradiated control sample.

386 The inhibition growth of *R. subcapitata* reached 32%, 13% and 20% at  $\text{UV}_{254}$  doses of 864, 2356  
387 and  $4712 \text{ mJ}\cdot\text{cm}^{-2}$  respectively (Fig. 4), thus confirming an acute **toxicological** effect on the  $\text{UV}_{254}$   
388 only treated samples. In contrast, a small reduction of the inhibition growth was observed for the  
389 samples **treated with  $\text{UV}_{254}/\text{H}_2\text{O}_2$**  at increasing  $\text{UV}_{254}$  doses, **which supported** the beneficial  
390 effect of the  $\text{H}_2\text{O}_2$  assisted photolytic treatment for toxicity reduction.

391 The results showed an increase of **the production of ROS** in all samples, that **could** enhance **the**  
392 sublethal toxicity in daphnids. **Aquatic organisms can in fact** adapt to **an increase of ROS**  
393 production by upregulating the **activity** of their antioxidant enzymes, **particularly of CAT** and  
394 **SOD which represent** the first and the second line of defense against ROS (Oexle et al., 2016). An  
395 evident increase of ROS production in **the daphnids treated with  $\text{UV}_{254}$  only samples was observed**  
396 **in comparison to the those** treated **with the  $\text{UV}_{254}/\text{H}_2\text{O}_2$  samples** (Fig. 5A). The increase was

397 recorded for UVC doses of 864 and 2356  $\text{mJ}\cdot\text{cm}^{-2}$  **for the**  $\text{UV}_{254}$  process and **at** 280  $\text{mJ}\cdot\text{cm}^{-2}$  **for the**  
398 samples treated **with**  $\text{UV}_{254}/\text{H}_2\text{O}_2$ .

399 The SOD activity resulted in significant alterations only for samples treated by  $\text{UV}_{254}$  (Fig. 5B).

400 The enzyme inhibition increased when **the** UVC dose was increased **and reached** the highest  
401 inhibition at 2356  $\text{mJ}\cdot\text{cm}^{-2}$ . No effect was observed in **the** samples treated **with**  $\text{UV}_{254}/\text{H}_2\text{O}_2$  except  
402 for samples treated with **a** UVC dose of 280  $\text{mJ}\cdot\text{cm}^{-2}$  (**TOC removal degree: 28%**).

403 Both processes led to a significant increase of CAT activity compared to **the** control (Fig. 5C), since  
404 CAT is responsible for the detoxification of high levels of hydrogen peroxide, one of the most  
405 important ROS producers under oxidative stress conditions.

406 On the contrary, GST activity remained unchanged or decreased **with** both treatments as shown in  
407 Figure 5D. Probably the response patterns may be species-specific in nature, while varying in  
408 intensity response. The antioxidant enzymes can maintain cellular redox balance, alleviate the  
409 **toxicological** effects of ROS and protect **the** cells against **the** oxidative damage of **their** structures  
410 including lipid, membranes, proteins and nucleic acids (Oropesa et al., 2017).

411 A 21 days chronic exposure experiment was performed to determine the toxicity of 100 fold diluted  
412 untreated and treated solutions. The effects of ACY (120  $\mu\text{g}\cdot\text{L}^{-1}$ ) and its treated samples on *D.*  
413 *magna* reproduction and survival are reported in Figure 6A,B.

414 The results of chronic toxicity showed that the  $\text{UV}_{254}$  treatment, even at such low concentrations of  
415 ACY, significantly decreased the survival of *D. magna* compared to the control group. A decrease  
416 of survival was further recorded for samples exposed at a **TOC removal of less than 5%** (ACY  
417 conversion degree: 45%), probably due the presence of unconverted ACY, and at  $\text{UV}_{254}$  dose of  
418 2356  $\text{mJ}\cdot\text{cm}^{-2}$  (ACY conversion: 90%), due to the formation of first-generation-transformation by-  
419 products **structurally similar to ACY**. At higher  $\text{UV}_{254}$  doses (4712  $\text{mJ}\cdot\text{cm}^{-2}$ , **TOC removal ~**  
420 **5%**), the survival percentage was similar to that of the control samples and always higher to that of  
421 the untreated sample. On the contrary, the ecotoxicity assessment for the  $\text{UV}_{254}/\text{H}_2\text{O}_2$  treated

422 solutions reflected the results already recorded in the acute tests, revealing a marked reduction of  
423 chronic toxic effects for the exposures of the daphnids to the UV<sub>254</sub>/H<sub>2</sub>O<sub>2</sub> samples, especially the  
424 highest UV<sub>254</sub> doses (**950 mJ·cm<sup>-2</sup>, TOC removal 77% and 1900 mJ·cm<sup>-2</sup>, TOC removal higher**  
425 **than 95%**).

426 As reported in Table 3, the reproduction of *D. magna* was completely inhibited in the organisms  
427 contacted with samples exposed to UV<sub>254</sub> doses of 864 mJ·cm<sup>-2</sup> and 2356 and in absence of H<sub>2</sub>O<sub>2</sub>.  
428 These results revealed that all the endpoints were different than the control solutions with an  
429 extended exposure to the treatment, thus confirming that the photoproducts formed during UV<sub>254</sub>  
430 irradiation of aqueous ACY solutions exerted significant chronic adverse effects to *D. magna* at the  
431 population level. On the contrary, the total number of neonates and the number of first-brood were  
432 not statistically different among the samples untreated and treated by UV<sub>254</sub>/H<sub>2</sub>O<sub>2</sub>.

433 **The different chemical species formed during the UV<sub>254</sub> and the UV<sub>254</sub>/H<sub>2</sub>O<sub>2</sub> photochemical**  
434 **processes could reasonably explain the observed toxicological effects. To provide a**  
435 **preliminary validation of this hypothesis, two samples, one from UV<sub>254</sub> photolysis and the**  
436 **second from UV<sub>254</sub>/H<sub>2</sub>O<sub>2</sub> treatment, were directly analyzed with MS-spectrometer to identify**  
437 **the main chemical intermediates formed, with the knowledge that a thorough identification of**  
438 **the transformation by-products required more sophisticated diagnostic techniques**  
439 **(Buchberger, 2011).**

440 **A list of molecular structures of the main intermediates that could be attributed to some**  
441 **peaks detected in the mass spectra for two samples is reported in Table 4. Some of the**  
442 **structures shown in Table 4 correspond to the chemical intermediates previously detected and**  
443 **reported in literature. In particular, for the UV<sub>254</sub> photolysis, the structures II, IV and V**  
444 **were observed during the degradation of ACY by TiO<sub>2</sub> photocatalysis at 365 nm (An et al.,**  
445 **2015) whereas the by-products VII and X proposed for UV<sub>254</sub>/H<sub>2</sub>O<sub>2</sub> were the same of those**  
446 **observed during the photooxidation of ACY in phosphate buffer at wavelength higher than**  
447 **270 nm (Iqbal et al., 2005).. The attribution of reliable structures to the remaining recorded**

448 **MS signals not previously observed by others, needs further analytical assessments. However,**  
449 **although an uncomplete analysis is available for the products of degradation of ACY, the data**  
450 **collected indicated the presence of chemical species significantly different in the two samples.**  
451 **In particular, UV<sub>254</sub>/H<sub>2</sub>O<sub>2</sub> process seems to lead mainly to the formation of hydroxylated**  
452 **imidazole-based compounds or species formed by the fragmentation of the pyrimidine ring**  
453 **whereas some hydroxylated ACY based intermediates are detected in the UV<sub>254</sub> treated**  
454 **sample.**

455

## 456 **5. Conclusion**

457 The photodegradation of ACY was investigated under UV<sub>254</sub> irradiation in the absence and in the  
458 presence of hydrogen peroxide. A moderate rate of direct photolysis at 254 nm for ACY was  
459 observed with a quantum yield of  $(1.62 \pm 0.073) \cdot 10^{-3} \text{ mol} \cdot \text{ein}^{-1}$  in the pH range 4.5 – 8.0. An  
460 average value of  $1.76 \cdot 10^9 \text{ M}^{-1} \cdot \text{s}^{-1}$  was calculated for the kinetic constant of reaction between  
461 hydroxyl radical and ACY. Considering (i) the UV<sub>254</sub> doses typically used for the disinfection of  
462 municipal sewage treatment plant effluents, (ii) the concentration values of ACY measured in  
463 WWTP effluents, and (iii) the results collected during the kinetic and ecotoxicity assessment, the  
464 occurrence of residual photodecomposition by-products in treated effluents is very likely, and these  
465 are likely to have a high ecotoxicological index. However, the addition of appropriate amount of  
466 hydrogen peroxide during the UV<sub>254</sub> disinfection stage would reduce this risk.

467 The results obtained contribute to provide useful information for a vision about the fate of ACY  
468 during the UV<sub>254</sub> and UV<sub>254</sub>/H<sub>2</sub>O<sub>2</sub> treatment processes and the eventual associated risks for living  
469 organisms (animals and plants) in the aquatic environment.

470 The results collected confirm the use of oxidative stress biomarkers as promising tool in order to  
471 evaluate the toxicological effects of environmental pollutants as early indicators in ecotoxicology.  
472 Exposure to environmental pollutants may disrupt the balance of biological oxidant-to-antioxidant  
473 ratio in aquatic species leading to elevated levels of ROS and resulting in oxidative stress. **A**

474 **preliminary analysis on the treated samples indicated, as the main photo-transformation by-**  
475 **products, the presence of hydroxylated ACY based intermediates in the UV<sub>254</sub> treatment**  
476 **process, and hydroxylated imidazole based compounds or species formed by the**  
477 **fragmentation of the pyrimidine ring in the UV<sub>254</sub>/H<sub>2</sub>O<sub>2</sub> treatment process.**

478 Further efforts are required to identify the main photoproducts, to elucidate the mechanism of ACY  
479 photodegradation under UVC radiation and to evaluate possible cumulative effects of the different  
480 species occurring in STP effluents.

481

## 482 **Acknowledgements**

483 The Authors are grateful to ERASMUS-Mobility Student Program, and to Ing. Giulio Di Costanzo  
484 for his precious support during the experimental campaign.

485

## 486 **References**

487 **Aebi, H., (1984) Catalase in vitro. *Methods in Enzymology* 6, 105–121.**

488 An, T., An, J., Gao, Y., Li, G., Fang, H., Song, W. (2015) Photocatalytic degradation and  
489 mineralization mechanism and toxicity assessment of antiviral drug acyclovir: Experimental and  
490 theoretical studies. *Applied Catalysis B: Environmental* 164, 279–287.

491 Asano, T. (1998) Wastewater Reclamation and Reuse, in *Water Quality Management Library*, Vol  
492 10. C.R.C. Press, Boca Raton.

493 Azuma, T., Arima, N., Tsukada, A., Hirami, S., Matsuoka, R., Moriwake, R., Ishiuchi, H., Inoyama,  
494 T., Teranishi, Y., Yamaoka, M., Mino, Y., Hayashi, T., Fujita, Y., Masada, M. (2016) Detection of  
495 pharmaceuticals and phytochemicals together with their metabolites in hospital effluents in Japan,  
496 and their contribution to sewage treatment plant influents. *Science of the Total Environment* 548–  
497 549, 189–197.

498 Bielski, B.H., Cabelli, D.E., Aruda, R.L., Ross, A.B. (1985) Reactivity of HO<sub>2</sub>/O<sub>2</sub> radicals in  
499 aqueous solution. *Journal of Physical and Chemical Reference Data* 14, 1041-1077.

500 Bradford, M.M. (1976) A rapid and sensitive method for the quantitation of microgram quantities of  
501 protein utilizing the principle of protein-dye binding. *Anal. Biochem.* 72, 248–254.

502 Bradley, P.M., Barber, L.B., Duris, J.W., Foreman, W.T., Furlong, E.T., Hubbard, L.E.,  
503 Hutchinson, K.J., Keefe, S.H., Kolpin, D.W. (2014) Riverbank filtration potential of  
504 pharmaceuticals in a wastewater-impacted stream. *Environmental Pollution* 193, 173–180.

505 Bryan-Marrugo, O.L., Ramos-Jiménez, J., Barrera-Saldana, H., Rojas-Martínez, A., Vidaltamayo,  
506 R., Rivas-Estilla, A.M. (2015) History and progress of antiviral drugs: From acyclovir to direct-  
507 acting antiviral agents (DAAs) for Hepatitis C. *Medicina Universitaria* 17(68), 165–174.

508 **Buchberger, W.W. (2011) Current approaches to trace analysis of pharmaceuticals and**  
509 **personal care products in the environment. *Journal of Chromatography A* 1218, 603–618.**

510 Buxton, G.V., Greenstock, C.L., Helman, W.P., Ross, A.B. (1988) Critical review of rate constants  
511 for reactions of hydrated electrons, hydrogen atoms and hydroxyl radicals (OH/O) in aqueous  
512 solution. *Journal of Physical and Chemical Reference Data* 17, 513–886.

513 Canonica, S., Meunier, L., von Gunten, U. (2008) Phototransformation of selected pharmaceuticals  
514 during UV treatment of drinking water. *Water Research* 42, 121–128.

515 **Conner-Kerr, T.A., Sullivan, P.K., Gaillard, J., Franklin, M.E., Jones, R.M. (1998) The effects**  
516 **of ultraviolet radiation on antibiotic-resistant bacteria in vitro. *Ostomy Wound Manage.* 44,**  
517 **50–56.**

518 **Crapo, J.D., McCord, J.M., Fridovich, I. (1978) Preparation and assay of superoxide**  
519 **dismutases. *Methods in Enzymology* 53, 382–393.**

520 Crespo-Hernandez, C.E., Flores, S., Torres, C., Negron-Encarnacion, I., Arce, R. (2000a) Part I.  
521 Photochemical and photophysical studies of guanine derivatives: intermediates contributing to its  
522 photodestruction mechanism in aqueous solution and the participation of the electron adduct.  
523 *Photochemistry and Photobiology* 71(5), 534–543.

524 Crespo-Hernandez, C.E., Arce, R. (2000b) Part II. Mechanism of formation of guanine as one of the  
525 major products in the 254 nm photolysis of guanine derivatives: concentration and pH effects.  
526 *Photochemistry and Photobiology* 71(5), 544–550.

527 Da Silva, L.M., Cavalcante, R.P., Cunha, R.F., Gozzi, F., Dantas, R.F., De Oliveira, S.C.,  
528 Machulek, A.J. (2016) Tolfenamic acid degradation by direct photolysis and the UV-ABC/H<sub>2</sub>O<sub>2</sub>  
529 process: factorial design, kinetics, identification of intermediates, and toxicity evaluation. *Science*  
530 *of the Total Environment* 573, 518–531.

531 DVGW, 1997. W 294. UV-Desinfektionsanlagen für die Trinkwasserversorgung-Anforderungen  
532 und Prüfung.

533 **FDA (Food and Drug Administration). Guidance for Industry: Environmental Assessment of**  
534 **Human Drug and Biologics Application. CDER/CBER CMC 6, rev 1, 39 pp, July 1998.**  
535 **Available: <http://www.fda.gov/cber/guidelines.htm>.**

536 Florence, A. T. (2010) *An Introduction to Clinical Pharmaceutics*. Ed. Pharmaceutical Press,  
537 London.

538 Funke, J., Prasse, C., Ternes, T.A. (2016) Identification of transformation products of antiviral  
539 drugs formed during biological wastewater treatment and their occurrence in the urban water cycle.  
540 *Water Research* 98, 75–83.

541 Galdiero, E., Siciliano, A., Maselli, V., Gesuele, R., Guida, M., Fulgione, D., Galdiero, S.,  
542 Lombardi, L., Falanga, A. (2016) An integrated study on antimicrobial activity and ecotoxicity of  
543 quantum dots and quantum dots coated with the antimicrobial peptide indolicidin. *International*  
544 *Journal of Nanomedicine* 11, 4199–4211.

545 García-Galan, M. J., Anfruns, A., Gonzalez-Olmos, R., Rodriguez-Mozaz, S., Comas, J. (2016)  
546 Advanced oxidation of the antibiotic sulfapyridine by UV/H<sub>2</sub>O<sub>2</sub>: Characterization of its  
547 transformation products and ecotoxicological implications. *Chemosphere* 147, 451–459.

548 Gillman, A., Nykvist, M., Muradrasoli, S., Soderstrom, H., Wille, M., Daggfeldt, A., Brojer, C.,  
549 Waldenstrom, J., Olsen, B., Jarhult, J.D. (2015) Influenza A(H7N9) virus acquires resistance-

550 related neuraminidase I222T substitution when infected mallards are exposed to low levels of  
551 oseltamivir in water. *Antimicrobial Agents and Chemotherapy* 59(9), 5196–5202.

552 Goldstein, S., Aschengrau, D., Diamant, Y., Rabani, J. (2007) Photolysis of aqueous H<sub>2</sub>O<sub>2</sub>:  
553 quantum yield and applications for polychromatic UV actinometry in photoreactors. *Environmental*  
554 *Science & Technology* 41, 7486-7490.

555 Guo, M.T., Yuan, Q.B., Yang, J. (2013) Ultraviolet reduction of erythromycin and  
556 tetracyclineresistant heterotrophic bacteria and their resistance genes in municipal wastewater.  
557 *Chemosphere* 93, 2864–2868.

558 **Habig, W.H., Pabst, M.J., Jakoby, W.B. (1974) Glutathione-S-transferases. The first step in**  
559 **mercapturic acid formation. *Journal of Biological Chemistry* 249, 7130–7139.**

560 Hijnen, W.A.M., Beerendonk, E.F., Medema, G.J. (2006) Inactivation credit of UV radiation for  
561 viruses, bacteria and protozoan (oo)cysts in water: a review. *Water Research* 40 (1), 3–22.

562 Hill, A., Khoo, S., Fortunak, J., Simmons, B., Ford, N. (2014) Minimum costs for producing  
563 hepatitis C direct-acting antivirals for use in large-scale treatment access. *Programs in Developing*  
564 *Countries. Clinical Infectious Diseases* 58(7), 928–936.

565 Hoekstra, A.Y. (2014) Water scarcity challenges to business. *Nature Climate Change* 4, 318–322.

566 **Huang, J.J., Hu, H.Y., Tang, F., Li, Y., Lu, S.Q. Lu, Y. (2011) Inactivation and reactivation of**  
567 **antibiotic-resistant bacteria by chlorination in secondary effluents of a municipal wastewater**  
568 **treatment plant. *Water Research* 45, 2775–2781.**

569 **Iqbal, J., Husain, A., Gupta, A. (2005) Photooxidation of acyclovir in aqueous solution.**  
570 ***Pharmazie* 60(8), 574–576**

571 ISO 6341:2013 Water quality: determination of the inhibition of the mobility of *Daphnia magna*  
572 Straus (Cladocera, Crustacea) acute toxicity test.

573 ISO 8692:2012 Water quality: fresh water algal growth inhibition test with unicellular green algae.



574 ISO 11348-3:2007 Water quality: determination of the inhibitory effect of water samples on the  
575 light emission of *Vibrio fischeri* (Luminescent bacteria test), part 3: method using freeze-dried  
576 bacteria.

577 Jain, S., Kumar, P., Vyas, R.K., Pandit, P., Dalai, A.K. (2013) Occurrence and removal of antiviral  
578 drugs in environment: A review. *Water, Air, & Soil Pollution* 224, 1410–1419.

579 Khan, S., Beattie, T.K., Knapp, C.W. (2016) Relationship between antibiotic- and disinfectant-  
580 resistance profiles in bacteria harvested from tap water. *Chemosphere* 152, 132–141.

581 Kim, I., Yamashita, N., Tanaka, H. (2009) Photodegradation of pharmaceuticals and personal care  
582 products during UV and UV/H<sub>2</sub>O<sub>2</sub> treatments. *Chemosphere* 77, 518–525.

583 Kovacic, M., Perisic, D.J., Biosic, M., Kusic, H., Babic, S., Bozic, A.L. (2016) UV photolysis of  
584 diclofenac in water; kinetics, degradation pathway and environmental aspects. *Environmental*  
585 *Science and Pollution Research* 23, 14908–14917.

586 Liu, W.R., Ying, G.G., Zhao, J.L., Liu, Y.S., Hu, L.X., Yao, L., Liang, Y.Q., Tian, F. (2016)  
587 Photodegradation of the azole fungicide climbazole by ultraviolet irradiation under different  
588 conditions: Kinetics, mechanism and toxicity evaluation. *Journal of Hazardous Materials* 318, 794–  
589 801.

590 **Lofrano, G., Libralato, G., Adinolfi, R., Siciliano, A., Iannece, P., Guida, M., Giugni, M.,**  
591 **Volpi Ghirardini, A., Carotenuto, M. (2016) Photocatalytic degradation of the antibiotic**  
592 **chloramphenicol and its by-products toxicity effects. *Ecotoxicology and Environmental Safety***  
593 **123, 65–71..**

594 Ma, J., Lv, W., Chen, P., Lu, Y., Wang, F., Li, F., Yao, K., Liu, G. (2016) Photodegradation of  
595 gemfibrozil in aqueous solution under UV irradiation: kinetics, mechanism, toxicity, and  
596 degradation pathways. *Environmental Science and Pollution Research* 23, 14294–14306.

597 Marotta, R., Spasiano, D., Di Somma, I., Andreozzi, R. (2013) Photodegradation of naproxen and  
598 its photoproducts in aqueous solution at 254 nm: a kinetic investigation. *Water Research* 47, 373–  
599 383.

600 McCurry, D.L., Bear, S.E., Bae, J., Sedlak, D.L., McCarty, P.L., Mitch, W.A. (2014) Superior  
601 removal of disinfection byproduct precursors and pharmaceuticals from wastewater in a staged  
602 anaerobic fluidized membrane bioreactor compared to activated sludge. *Environmental Science &  
603 Technology Letters* 1, 459–464.

604 **Meckes, M.C. (1982) Effect of UV light disinfection on antibiotic-resistant coliforms in  
605 wastewater effluents. *Appl. Environ. Microbiol.* 43, 371–377.**

606 Montemayor, M., Costan, A., Lucena, F., Jofre, J., Munoz, J., Dalmau, E., Mujeriego, R., Salas L.  
607 (2008) The combined performance of UV light and chlorine during reclaimed water disinfection.  
608 *Water Science & Technology* 57(6), 935–940.

609 **Munir, M., Wong, K., Xagorarakis, I. (2011) Release of antibiotic resistant bacteria and genes  
610 in the effluent and biosolids of five wastewater utilities in Michigan. *Water Research* 45, 681–  
611 693.**

612 Nick, K., Scholer, H.F., Mark, G., Soylemez, T., Akhlaq, M.S., Schuchmann, H.P., von Sonntag, C.  
613 (1992) Degradation of some triazine herbicides by UV radiation such as used in the UV disinfection  
614 of drinking water. *Journal of Water Supply: Research and Technology Aqua* 41(2), 82–87

615 Nicole, I., De Laat, J., Doré, M., Duguet, J.P., Bonnel, C. (1990) Use of UV radiation in water  
616 treatment: measurement of photonic flux by hydrogen peroxide actinometry. *Water Research* 24,  
617 157-168.

618 NWRI (2012) Ultraviolet Disinfection: Guidelines for Drinking Water and Water Reuse, Third  
619 Edition. Published by National Water Research Institute.

620 OECD (2012) Guidelines for Testing of Chemicals. *Daphnia magna* Reproduction Test. OECD 211.  
621 Paris, France.

622 Oexle, S., Jansen, M., Pauwels, K., Sommaruga, M., De Meester, L., Stoks, R. (2016) Rapid  
623 evolution of antioxidant defence in a natural population of *Daphnia magna*. *Journal of Evolutionary  
624 Biology* 29, 1328–1337.

625 ONorm, M. (2001). Anlagen zur Desinfektion von Wasser mittels Ultraviolett-Strahlen.  
626 Anforderungen und Prufung 5873–1.

627 Onstein, P., Stefan, M.I., Bolton, J.R. (1999) Competition kinetics method for the determination of  
628 rate constants for the reaction of hydroxyl radicals with organic pollutants using the UV/H<sub>2</sub>O<sub>2</sub>  
629 advanced oxidation technology: the rate constants for the tert-buthylformate ester and 2,4-  
630 dinitrophenol. Journal of Advanced Oxidation Technologies 4(2), 231–236.

631 **Organisation for Economic Cooperation and development (OECD), 1999. Guidelines for**  
632 **testing of chemicals, simulation test-aerobic sewage treatment, 303A.**

633 Oropesa, A.L., Novais, S.C., Lemos, M.F.L. Espejo, A., Gravato, C., Beltran, F. (2017) Oxidative  
634 stress response of *Daphnia magna* exposed to effluents spiked with emerging contaminants under  
635 ozonation and advanced oxidation process. Environmental Science & Pollution Research 24, 1735–  
636 1747.

637 Peng, X., Wang, C., Zhang, K., Wang, Z., Huang, Q., Yu, Y., Ou, W. (2014) Profile and behavior  
638 of antiviral drugs in aquatic environments of the Pearl River Delta, China. Science of the Total  
639 Environment 466–467, 755–761.

640 Pereira, V.J., Weinberg, H.S., Linden, K.G., Singer, P.C. (2007) UV degradation of pharmaceutical  
641 compounds in surface water via direct and indirect photolysis at 254 nm. Environmental Science &  
642 Technology 41(5), 1682–1688.

643 Prasse, C., Schlusener, M.P., Schulz, R., Ternes, T.A. (2010) Antiviral drugs in wastewater and  
644 surface waters: A new pharmaceutical class of environmental relevance? Environmental Science &  
645 Technology 44, 1728–1735.

646 Prasse, C., Wagner, M., Schulz, R., Ternes, T.A. (2011) Biotransformation of the antiviral drugs  
647 acyclovir and penciclovir in activated sludge treatment. Environmental Science &  
648 Technology 45(7), 2761–2769.

649 Prasse, C., Wenk, J., Jasper, J.T., Ternes, T.A., Sedlak, D.L.(2015) Co-occurrence of photochemical  
650 and microbiological transformation processes in open-water unit process wetlands. *Environmental*  
651 *Science & Technology* 49, 14136–14145.

652 Reis, N.M., Li Puma, G. (2015) Novel microfluidics approach for extremely fast and efficient  
653 photochemical transformations in fluoropolymer microcapillary films. *ChemicalCommunications*  
654 51, 8414–8417.

655 Richardson, S.D. (2012) Environmental mass spectrometry: emerging contaminants and current  
656 issues. *Analytical Chemistry* 84, 747–778.

657 Richardson, S.D., Plewa, M.J., Wagner, E.D., Schoeny, R., DeMarini, D.M. (2007) Occurrence,  
658 genotoxicity, and carcinogenicity of regulated and emerging disinfection by-products in drinking  
659 water: a review and roadmap for research. *Mutation Research* 636(1-3), 178-242.

660 Rozas, O., Vidal, C., Baeza, C., Jardim, W.F., Rossner, A., Mansilla, H.D. (2016) Organic  
661 micropollutants (OMPs) in natural waters: Oxidation by UV/H<sub>2</sub>O<sub>2</sub> treatment and toxicity  
662 assessment. *Water Research* 98, 109–118.

663 Russo, D., Spasiano, D., Vaccaro, M., Andreozzi, R., Li Puma, G., Reis, N.M., Marotta, R. (2016)  
664 Direct photolysis of benzoylecgonine under UV irradiation at 254 nm in a continuous flow  
665 microcapillary array photoreactor. *Chemical Engineering Journal* 283, 243–250.

666 Sanderson, H., Johnson, D.J., Reitsma, T., Brain, R.A., Wilson, C.J., Solomon, K.R. (2004)  
667 Ranking and prioritization of environmental risks of pharmaceuticals in surface waters. *Regulatory*  
668 *Toxicology and Pharmacology* 39(2), 158–183.

669 **Shi, P., Jia, S., Zhang, X.X., Zhang, T., Cheng, S., Li, A. (2013) Metagenomic insights into**  
670 **chlorination effects on microbial antibiotic resistance in drinking water. *Water Research* 47,**  
671 **111–120.**

672 Singer, A.C., Nunn, M.A., Gould, E.A., Johnson, A.C. (2007) Potential risks associated with the  
673 proposed widespread use of Tamiflu. *Environmental Health Perspectives* 115(1), 102–106.

674 Sinha, V.R., Monika, Trehan, A., Kumar, M., Singh, S., Bhinge, J.R. (2007) Stress studies on  
675 Acyclovir. *Journal of Chromatographic Science* 45, 319–324.

676 Spasiano, D., Russo, D., Vaccaro, M., Siciliano, A., Marotta, R., Guida, M., Reis, N.M., Li Puma,  
677 G., Andreozzi, R. (2016) Removal of benzoylecgonine from water matrices through UV<sub>254</sub>/H<sub>2</sub>O<sub>2</sub>  
678 process: reaction kinetic modeling, ecotoxicity and genotoxicity assessment. *Journal of Hazardous*  
679 *Materials* 318, 515–525.

680 Yuan, F., Hu, C., Hu, X., Wei, D., Chen, Y., Qu, J. (2011) Photodegradation and toxicity changes  
681 of antibiotics in UV and UV/H<sub>2</sub>O<sub>2</sub> process. *Journal of Hazardous Materials* 185, 1256–1263.

682 Zhou, C., Chen, J., Xie, Q., Wei, X., Zhang, Y., Fu, Z. (2015) Photolysis of three antiviral drugs  
683 acyclovir, zidovudine and lamivudine in surface freshwater and seawater. *Chemosphere* 138, 792–  
684 797.

1 **Photodegradation and ecotoxicology of acyclovir in water under UV<sub>254</sub> and**  
2 **UV<sub>254</sub>/H<sub>2</sub>O<sub>2</sub> processes**

3

4 Danilo Russo<sup>a</sup>, Antonietta Siciliano<sup>b</sup>, Marco Guida<sup>b</sup>, Emilia Galdiero<sup>b</sup>, Angela Amoresano<sup>c</sup>,  
5 Roberto Andreozzi<sup>a</sup>, Nuno M. Reis<sup>d,e</sup>, Gianluca Li Puma<sup>e,‡</sup> and Raffaele Marotta<sup>a,†</sup>

6

7 <sup>a</sup> Dipartimento di Ingegneria Chimica, dei Materiali e della Produzione Industriale, Università di  
8 Napoli Federico II, p.le V. Tecchio 80, Napoli, Italy.

9 <sup>b</sup> Dipartimento di Biologia, Università di Napoli Federico II, Complesso Universitario Monte  
10 Sant'Angelo, via Cinthia 4, Napoli, Italy.

11 <sup>c</sup> Dipartimento di Scienze Chimiche, Università di Napoli Federico II, Complesso Universitario  
12 Monte Sant'Angelo, via Cinthia 4, Napoli, Italy.

13 <sup>d</sup> Department of Chemical Engineering, University of Bath, Claverton Down, Bath BA2 7AY, UK.

14 <sup>e</sup> Environmental Nanocatalysis & Photoreaction Engineering Department of Chemical Engineering,  
15 Loughborough University, Loughborough LE11 3TU, UK.

16

17 <sup>†</sup> *Corresponding author:* Tel.: +39(0)817682968, fax: +39815936936. E-mail address:  
18 rmarotta@unina.it (R. Marotta).

19 <sup>‡</sup> *Corresponding author:* Tel.: +44(0)1509222510, fax: +44(0)1509223923. E-mail address:  
20 G.Lipuma@lboro.ac.uk (G. Li Puma).

21

22 **Abstract**

23 The photochemical and ecotoxicological fate of acyclovir (ACY) through UV<sub>254</sub> direct photolysis  
24 and in the presence of hydroxyl radicals (UV<sub>254</sub>/H<sub>2</sub>O<sub>2</sub> process) were investigated in a microcapillary  
25 film (MCF) array photoreactor, which provided ultrarapid and accurate photochemical reaction

26 kinetics. The UVC phototransformation of ACY was found to be unaffected by pH in the range  
27 from 4.5 to 8.0 and resembled an apparent autocatalytic reaction. The proposed mechanism  
28 included the formation of a photochemical intermediate ( $\phi_{ACY} = (1.62 \pm 0.07) \cdot 10^{-3} \text{ mol-ein}^{-1}$ ) that  
29 further reacted with ACY to form by-products ( $k' = (5.64 \pm 0.03) \cdot 10^{-3} \text{ M}^{-1} \cdot \text{s}^{-1}$ ). The photolysis of  
30 ACY in the presence of hydrogen peroxide accelerated the removal of ACY as a result of formation  
31 of hydroxyl radicals. The kinetic constant for the reaction of OH radicals with ACY ( $k_{OH/ACY}$ )  
32 determined with the kinetic modeling method was  $(1.23 \pm 0.07) \cdot 10^9 \text{ M}^{-1} \cdot \text{s}^{-1}$  and with the  
33 competition kinetics method was  $(2.30 \pm 0.11) \cdot 10^9 \text{ M}^{-1} \cdot \text{s}^{-1}$  with competition kinetics. The acute and  
34 chronic effects of the treated aqueous mixtures on different living organisms (*Vibrio fischeri*,  
35 *Raphidocelis subcapitata*, *D. magna*) revealed significantly lower toxicity for the samples treated  
36 with UV<sub>254</sub>/H<sub>2</sub>O<sub>2</sub> in comparison to those collected during UV<sub>254</sub> treatment. This result suggests that  
37 the addition of moderate quantity of hydrogen peroxide (30-150 mg·L<sup>-1</sup>) might be a useful strategy  
38 to reduce the ecotoxicity of UV<sub>254</sub> based sanitary engineered systems for water reclamation.

39

40 *Keywords:* UVC, hydrogen peroxide photolysis, microreactor, ecotoxicity, water reuse, acyclovir  
41 removal.

42

## 43 **1. Introduction**

44 Water reclamation and water reuse is becoming increasingly common in industrialized countries  
45 with high water demands and in water stressed regions characterized by considerable scarcity of  
46 freshwater (Hoekstra, 2014). The most common treatment method for water reuse is chlorination at  
47 typical dosages ranging from 5 to 20 mg/L with a maximum of two hours of contact time (Asano,  
48 1998). However, concerns related to (i) the adverse impacts of chlorine on irrigated crops, (ii) the  
49 high ecotoxicity of chlorinated by-products (DBPs) formed during the chlorination stage  
50 (Richardson et al., 2007) and (iii) the survival of antibiotics resistant bacteria during chlorination

51 (Khan et al., 2016) with a possible selection of some antibiotic resistance genes in the wastewater  
52 microbial community (Huang et al., 2011) should drive the transition from chlorine disinfection to  
53 other more ecofriendly suitable methods. UV radiation treatment (especially UVC,  $\lambda < 280$  nm)  
54 produces a high sterilization efficiency (Montemayor et al., 2008) and could represent a viable  
55 alternative to chlorination for the disinfection and reuse of effluents from wastewater treatment  
56 plant (WWTP) for irrigation (i.e., after membrane filtration and/or reverse osmosis) or for aquifer  
57 recharge. Numerous wastewater sites have adopted UVC treatment for effluents disinfection. For  
58 example, Florida and California have favored wastewater reuse and adopted specific regulations on  
59 reclamation technologies through UV disinfection processes. UVC doses (fluence) ranging from 50  
60  $\text{mJ}\cdot\text{cm}^{-2}$  to  $150 \text{mJ}\cdot\text{cm}^{-2}$  have been suggested to efficiently inactivate pathogens accounting for the  
61 variability in the effluent composition (NWRI, 2012), although German and Austrian regulations  
62 (DVGW,1997; ONorm, 2001) suggest the use of  $40 \text{mJ}\cdot\text{cm}^{-2}$  UVC fluence to eliminate a large  
63 variety of bacteria and viruses (Conner-Kerr et al., 1998). Even though UV disinfection has been  
64 reported highly effective in the reduction of antibiotic resistance bacteria (ARB), particularly in  
65 comparison to chlorination (Shi et al., 2013; Hijnen et al., 2006), other investigations have  
66 demonstrated that UV disinfection may not contribute to the significant reduction of selected ARB,  
67 such as tetracycline-and sulfonamide-resistant bacteria (Munir et al., 2011; Meckes, 1982) thus  
68 indicating a plausible selectivity of UV on ARB (Guo et al., 2013).

69 Moreover, numerous studies have suggested that under the recommended UVC doses several  
70 biorefractory xenobiotics, particularly pharmaceuticals and personal care products generally  
71 occurring in municipal discharges and partially removed in WWTPs, may undergo photochemical  
72 transformations induced by UVC irradiation (Canonica et al., 2008; Nick et al., 1992; Pereira et al,  
73 2007; Kim et al., 2009; Ma et al., 2016; Kovacic et al., 2016; Liu et al., 2016; Marotta et al., 2013)  
74 which may generate by-products with high ecotoxicity (Rozas et al., 2016; Yuan et al., 2011). For  
75 these reasons, the use of hydrogen peroxide during UVC disinfection ( $\text{UV}_{254}/\text{H}_2\text{O}_2$ ) which produces  
76 highly reactive radical species, has been proposed as a viable treatment for effective removal of



77 micropollutant and ARB and, in consequence, for the reduction of the ecotoxicity risk (García-  
78 Galan et al., 2016; Melo da Silva et al., 2016).

79 Among the emerging Pharmaceuticals and Personal Care Products detected in WWTP effluents,  
80 antiviral drugs play a leading role (Richardson, 2012; Jain et al., 2013) due to their scarce  
81 biodegradability (Funke et al., 2016) and increased usage during the last decade, particularly for the  
82 treatment of viral diseases and for the prevention of pandemic outbreaks (Hill et al., 2014).  
83 Moreover, antiviral drugs have been considered as some of the most hazardous therapeutic  
84 substances exerting high toxicity towards biota, such as crustaceans, fish and algae (Sanderson et  
85 al., 2004). The presence of antiviral drugs in the environment raises considerable concern regarding  
86 their potential effect on the ecosystem, with the potential of developing antiviral drug resistance, in  
87 analogy to the development of antibiotic resistant bacteria (Singer et al., 2007; Gillman et al., 2015).  
88 Acyclovir (ACY) is one of the oldest and most widely used antiviral drug for treating two common  
89 viral infections (chickenpox-zoster and herpes simplex) and it is also prescribed to patients with  
90 weakened immune systems in order to control viral infections (i.e., viral conjunctivitis) (Bryan-  
91 Marrugo et al., 2015). ACY has been recently detected in different WWTP effluents as well as in  
92 surface water at level of few nanograms per liter up to over one micrograms per liter (Table 1).

93 The photodegradation pathways of ACY under artificial and natural solar light irradiation have been  
94 recently investigated (Zhou et al., 2015; Prasse et al., 2015). However, there is a lack of  
95 investigations on the photochemical transformation of ACY under  $UV_{254}$  and  $UV_{254}/H_2O_2$   
96 treatments and on the simultaneous ecotoxicological assessments of highly diluted treated solutions  
97 containing ACY.

98 More information is needed to determine the effectiveness of  $UV_{254}$  assisted processes on the  
99 removal of ACY from aqueous solutions and the impact that these processes may have on the  
100 structure of aquatic communities and on the ecosystem dynamics.

101 The use of microcapillary flow photoreactors has recently been proposed to intensify the treatment  
102 of substances that are either highly priced, scarcely commercially available or controlled substances

103 such as illicit drugs or selected pharmaceuticals (Reis and Li Puma, 2015; Russo et al., 2016). In  
104 contrast to conventional laboratory photochemical systems which require relatively larger volume  
105 of liquid, photochemical treatments in microphotoreactors are carried out in a highly controlled  
106 environment with minimal sample volumes (of the order of few mL), the sufficient amount to  
107 generate samples for subsequent analysis. Furthermore, photochemical transformations in  
108 microphotoreactors are executed at extremely short residence times (of the order of seconds) in  
109 comparison to conventional laboratory photoreactors, resulting in an efficient use of time and  
110 resources.

111 Under this background, in this study we investigated the degradation kinetics of ACY in distilled  
112 water under UV<sub>254</sub> and UV<sub>254</sub>/H<sub>2</sub>O<sub>2</sub> irradiation by means of a microcapillary film (MCF) array  
113 photoreactor and we evaluated the acute and chronic ecotoxicity of highly diluted treated samples  
114 using a range of selected organisms, to provide important information regarding the photolysis of  
115 ACY in UV<sub>254</sub> based sanitary engineered systems for water reclamation. The toxicity was assessed  
116 considering a battery of toxicity tests (*Aliivibrio fischeri*, *Raphidocelis subcapitata*, *Daphnia*  
117 *magna*) and endpoints (bioluminescence, growth inhibition, immobilization, survival, reproduction  
118 and biomarker) including three trophic and phylogenetic levels (Lofrano et al., 2016).

119 The battery of toxicity tests proposed were sensitive indicators of toxic pollutants, and also  
120 determined the great diversity of potential stress-receptor that could result from pharmaceuticals  
121 and their byproducts entering the environment (FDA, 1998).

122

## 123 **2. Materials and methods**

### 124 *2.1. Materials*

125 Hydrogen peroxide (30% v/v), ACY (pharmaceutical secondary standard), methanol ( $\geq 99.9\%$  v/v),  
126 formic acid ( $>99\%$  w/w), benzoic acid ( $\geq 99.5\%$  w/w), orthophosphoric acid (85% w/w in H<sub>2</sub>O),  
127 sodium hydroxide ( $>98\%$  w/w), perchloric acid (70% v/v), catalase from *Micrococcus lysodeikticus*  
128 and reagents for ecotoxicity tests were purchased from Sigma-Aldrich. An aqueous mixture of

129 peptone (32 ppm), meat extract (22 ppm), urea (6 ppm),  $K_2HPO_4$  (28 ppm),  $CaCl_2 \cdot H_2O$  (4 ppm),  
130 NaCl (7 ppm) and  $Mg_2SO_4$  (0.6 ppm) was used for the preparation of a synthetic wastewater  
131 according to the OECD Guidelines (Organisation for Economic Cooperation and  
132 development, 1999). The substances were purchased from Sigma-Aldrich and used as received.  
133 Milli-Q water was used as solvent in analytical determinations and experiments.

134

## 135 *2.2. Analytical methods*

136 The concentration of hydrogen peroxide, ACY, and benzoic acid was measured by HPLC (1100  
137 Agilent) equipped with a Gemini 5u C6-Phenyl 110 (Phenomenex) reverse phase column and a  
138 diode array detector. The mobile phase was a mixture of 93% aqueous orthophosphoric acid (10  
139 mM) and 7% methanol flowing at  $8.0 \cdot 10^{-4} \text{ L} \cdot \text{min}^{-1}$ . The pH of the aqueous solutions was adjusted  
140 with NaOH or  $HClO_4$  and measured with an Accumet Basic AB-10 pH-meter. The molar  
141 absorption coefficient of ACY was estimated using a Perkin Elmer UV/VIS spectrometer (mod.  
142 Lambda 35). Total organic carbon (TOC) was monitored by a TOC analyzer (Shimadzu 5000 A).  
143 MS analysis was performed by direct injection on Agilent 6230 TOF LC/MS coupled with Agilent  
144 HPLC system (1260 Series). The mobile phase was a mixture of methanol (10% v/v) and formic  
145 acid (0.1% v/v) aqueous solution at flow rate of  $0.4 \text{ mL} \cdot \text{min}^{-1}$  and the injection volume of samples  
146 was 20  $\mu\text{L}$ . The MS source was an electrospray ionization (ESI) interface in the positive ion mode  
147 with capillary voltage of 3500 V, gas temperature at 325  $^\circ\text{C}$ , dry gas ( $N_2$ ) flow at  $8 \text{ L} \cdot \text{min}^{-1}$  and the  
148 nebulizer at 35 psi. The MS spectra were acquired in a mass range of 100-3000 m/z with a rate of 1  
149 spectrum/s, time of 1000 ms/spectrum and transient/spectrum of 9905.

150

## 151 **3. Experimental apparatus and procedures**

### 152 *3.1. MCF array photoreactor*

153 The degradation kinetics of ACY by  $UV_{254}$  and  $UV_{254}/H_2O_2$  were investigated in a MCF array  
154 photoreactor described elsewhere (Reis et al., 2015; Russo et al., 2016). Briefly, the photoreactor

155 (Lamina Dielectrics Ltd) consisted of ten UV<sub>254</sub> transparent microcapillaries of fluorinated polymer  
156 characterized by a mean hydraulic diameter of 195 μm. The microcapillaries were coiled around a  
157 UV monochromatic (254 nm) lamp (Germicidal G8T5) in the region with uniform emission.  
158 Experiments were carried out at room temperature (~25 °C) in continuous flow through the reactor  
159 at different space times, using capillaries of different length exposed to the UV lamp irradiation.  
160 The flow rate through the MCF was  $6.0 \cdot 10^{-4} \text{ L} \cdot \text{min}^{-1}$ . Aqueous samples were collected from the  
161 MCF outlet, and rapidly analyzed by HPLC. At the end of each experimental run, the pH of the  
162 solutions was unchanged. The initial concentration of ACY used in the experiments ranged between  
163  $2.05 \cdot 10^{-5} \text{ mol} \cdot \text{L}^{-1}$  and  $4.67 \cdot 10^{-5} \text{ mol} \cdot \text{L}^{-1}$ .  
164 The lamp irradiance was varied by changing the nominal power from 4.5 W to 8.0 W using a  
165 variable power supply unit. The photon fluxes per unit volume emitted by the UV lamp ( $P_o$ ) for  
166 each power setting, estimated by H<sub>2</sub>O<sub>2</sub> actinometry (Nicole et al, 1990; Goldstein et al., 2007), were  
167  $1.92 \cdot 10^{-2} \text{ ein} \cdot (\text{s} \cdot \text{L})^{-1}$  (nominal power 8.0 W) and  $1.27 \cdot 10^{-2} \text{ ein} \cdot (\text{s} \cdot \text{L})^{-1}$  (nominal power 4.5 W). The  
168 MCF average optical path length ( $l_{MCF}$ ) was 154 μm. All the runs were carried out in duplicate. The  
169 data collected were used to estimate the kinetic unknown parameters (quantum yield of direct  
170 photolysis at 254 nm of ACY and kinetic constant of hydroxyl radical attack to ACY).

171

### 172 3.2. Cylindrical batch photoreactor

173 A cylindrical batch photoreactor ( $V_b = 0.480 \text{ L}$ ), equipped with a low-pressure mercury  
174 monochromatic lamp (Helios Italquartz, HGL10T5L, 17W nominal power emitting at 254 nm), was  
175 used to provide large sample volumes required for the ecotoxicity tests at varying treatment times  
176 (i.e., different UV<sub>254</sub> fluence). The UV<sub>254</sub> dose ( $\text{mJ} \cdot \text{cm}^{-2}$ ) was calculated as the average photon  
177 fluence rate multiplied by the treatment time. The average photon fluence rate emitted by the UV  
178 lamp at 254 nm was  $4.7 \text{ mW} \cdot \text{cm}^{-2}$  (UVC DELTA OHM radiometer). The experimental device was  
179 described elsewhere (Spasiano et al., 2016).

180

### 181 3.3. Ecotoxicity assessment

182 Reconstituted aqueous solution (pH =  $7.8 \pm 0.2$ ), was used as dilution water for cladoceran toxicity  
183 tests:  $\text{CaCl}_2 \cdot 2\text{H}_2\text{O}$  ( $290 \text{ mg} \cdot \text{L}^{-1}$ ),  $\text{MgSO}_4 \cdot 7\text{H}_2\text{O}$  ( $120 \text{ mg} \cdot \text{L}^{-1}$ ),  $\text{NaHCO}_3$  ( $65 \text{ mg} \cdot \text{L}^{-1}$ ),  $\text{KCl}$  ( $6$   
184  $\text{mg} \cdot \text{L}^{-1}$ ). Different salts were used for the preparation of algal test medium:  $\text{CaCl}_2 \cdot 2\text{H}_2\text{O}$  ( $18 \text{ mg} \cdot \text{L}^{-1}$ ),  
185  $\text{MgSO}_4 \cdot 7\text{H}_2\text{O}$  ( $15 \text{ mg} \cdot \text{L}^{-1}$ ),  $\text{NH}_4\text{Cl}$  ( $15 \text{ mg} \cdot \text{L}^{-1}$ ),  $\text{MgCl}_2 \cdot 6\text{H}_2\text{O}$  ( $12 \text{ mg} \cdot \text{L}^{-1}$ ),  $\text{KH}_2\text{PO}_4$  ( $1.6 \text{ mg} \cdot \text{L}^{-1}$ ),  
186  $\text{FeCl}_3 \cdot 6\text{H}_2\text{O}$  ( $0.08 \text{ mg} \cdot \text{L}^{-1}$ ),  $\text{Na}_2\text{EDTA} \cdot 2\text{H}_2\text{O}$  ( $0.1 \text{ mg} \cdot \text{L}^{-1}$ ),  $\text{H}_3\text{BO}_3$  ( $0.185 \text{ mg} \cdot \text{L}^{-1}$ ),  $\text{MnCl}_2 \cdot 4\text{H}_2\text{O}$   
187 ( $0.415 \text{ mg} \cdot \text{L}^{-1}$ ),  $\text{ZnCl}_2$  ( $0.003 \text{ mg} \cdot \text{L}^{-1}$ ),  $\text{CoCl}_2 \cdot 6\text{H}_2\text{O}$  ( $0.0015 \text{ mg} \cdot \text{L}^{-1}$ ),  $\text{Na}_2\text{MoO}_4 \cdot 2\text{H}_2\text{O}$  ( $7.0 \cdot 10^{-3}$   
188  $\text{mg} \cdot \text{L}^{-1}$ ),  $\text{CuCl}_2 \cdot 2\text{H}_2\text{O}$  ( $1.0 \cdot 10^{-5} \text{ mg} \cdot \text{L}^{-1}$ ). Reconstitution solution, osmotic adjusting solution (OAS)  
189 and diluent (NaCl 2%) were the reagents used in *Vibrio fischeri* toxicity test (Strategic diagnostics  
190 Inc. SDI).

191 The enzymatic assays chosen to evaluate oxidative stress were ROS (reactive oxygen species)  
192 content using 2,7- dichlorodihydrofluorescein ( $\text{H}_2\text{DCFDA}$ ) and activities of SOD (superoxide  
193 dismutase), CAT (catalase) and GST (glutathione transferase) that were measured using respective  
194 assay kits according to the manufacturer's instruction's (Sigma Aldrich). All determinations were  
195 quantified spectrophotometrically.

196 *V. fischeri*, *R. subcapitata* and acute *D. magna* assays were conducted with an initial ACY  
197 concentration of  $1.2 \text{ mg} \cdot \text{L}^{-1}$  and on its related  $\text{UV}_{254}$  and  $\text{UV}_{254}/\text{H}_2\text{O}_2$  treated solutions. Chronic  
198 toxicity and oxidative stress tests on *Daphnia magna* were performed starting on untreated and  
199 treated solutions diluted by 100 fold, in order to assess any differences at sub lethal concentration  
200 levels. Negative and positive controls were included in each experiment. The significance of  
201 differences of toxicity between the treated samples and controls was assessed by the analysis of  
202 variance (ANOVA) considering a significance threshold level always set at 5%. For higher variance  
203 than 5%, post-hoc tests were carried out with Dunnett's method and Tukey's test. Whenever

204 possible, toxicity was expressed as median effective concentration (EC<sub>50</sub>) with 95% confidence  
205 limit values. Otherwise, toxicity was expressed as percentage of effect (PE, %).

206

### 207 3.3.1. *Organisms maintenance and monitoring*

208 Freeze-dried *Vibrio fischeri* (strain NRRL-B-11177) cells were reconstituted with reagent diluent at  
209 4 °C. *Raphidocelis subcapitata* were cultured in ISO medium (ISO, 2012) at 23 ± 2 °C with  
210 continuous 4500 lux light and aeration (0.2 mm filtered air). *Daphnia magna* were cultured at 20 ±  
211 1 °C, with a 16:8 light/dark photoperiod in ISO water (ISO, 2012).

212 Luminescence *V. fischeri* measurements were performed with Microtox® Model 500 Toxicity  
213 Analyzer from Microbics Corporation (AZUR Environmental) equipped with a 30 well incubated at  
214 15 ± 1 °C and with excitation source at 490 nm wavelength.

215 *R. subcapitata* density was determined by an indirect procedure using a spectrophotometer (Hach  
216 Lange DR5000) and cuvette (5 cm). *D. magna* viability, mobility and growth were observed with a  
217 stereomicroscope (LEICA EZA-HD).

218

### 219 3.3.2. *Bacteria toxicity test*

220 The inhibitory effect of ACY samples on the light emission of *V. fischeri* (strain NRRL-B-11177)  
221 was evaluated with the 11348-3:2007 ISO method (ISO, 2007). Tests were carried out on an ACY  
222 concentration of 1.2 mg·L<sup>-1</sup> and on its related treated by-products solutions. OAS was added to each  
223 sample to ensure that the final NaCl concentration was above 2.0%. The initial light output from  
224 each cuvette containing reconstituted freeze-dried *V. fischeri* was recorded. The test solutions were  
225 then added and after 30 minutes exposure, the final light output was measured. Positive control tests  
226 for *V. fischeri* were carried out with C<sub>6</sub>H<sub>4</sub>Cl<sub>2</sub>O (EC<sub>50</sub> = 4.1 ± 2.2 mg·L<sup>-1</sup>).

227

### 228 3.3.3. *Algae toxicity test*

229 The *R. subcapitata* bioassay was conducted following the guidelines ISO 8692 (ISO, 2012). Three  
230 replicates were included for each sample. The replicates were inoculated with  $10^4$  algal cells·mL<sup>-1</sup>  
231 and incubated for 72 h at  $23 \pm 2$  °C under continuous illumination (irradiance range of 120-60  
232  $\mu\text{ein}\cdot\text{m}^{-2}\cdot\text{s}^{-1}$ ). The algal biomass exposed to the samples was compared with the algal biomass in the  
233 negative control. Positive control tests for *R. subcapitata* were carried out with K<sub>2</sub>Cr<sub>2</sub>O<sub>7</sub> (EC<sub>50</sub> =  $1 \pm$   
234  $0.2 \text{ mg}\cdot\text{L}^{-1}$ ).

235

#### 236 3.3.4. Crustaceans toxicity test

237 Acute toxicity tests with *D. magna* were carried out according to ISO 6341 (ISO, 2013). Newborn  
238 daphnids (<24 h old) were exposed in four replicates for 24 h and 48 h at  $20 \pm 1$  °C. Toxicity was  
239 expressed as percentage of immobilized organisms. Positive control tests for *D. magna* were carried  
240 out with K<sub>2</sub>Cr<sub>2</sub>O<sub>7</sub> (48h, EC<sub>50</sub> =  $0.6 \pm 0.1 \text{ mg}\cdot\text{L}^{-1}$ ).

241 The *D. magna* chronic bioassay was carried out according to the guideline OECD 211 (OECD,  
242 2012). Ten *D. magna* neonates (< 24 h hold) were used and individually placed for each treatment  
243 in beakers containing 50 ml of the test solutions, renewed every two other days. Organisms exposed  
244 for 21 days with ACY solutions were then fed one day with *R. subcapitata* ( $10^7$  cell·mL<sup>-1</sup>).  
245 Survival, reproduction and growth were observed daily, and newborns were discarded from  
246 beakers.

247 The amount of ROS produced in *D. magna* was determined using 2,7-dichlorodihydrofluorescein  
248 (H<sub>2</sub>DCFDA, Sigma Aldrich) using the method previously reported (Galdiero et al., 2016). After 48  
249 h of exposure, each exposed and not exposed living daphnids were rinsed with deionized water to  
250 remove any excess pharmaceuticals adhered to their body surface and transferred to a 96-well plate.  
251 A selected volume (200  $\mu\text{L}$ ) of 10 mM H<sub>2</sub>DCFDA was added to each well and the plate was then  
252 incubated for 4 h in the dark at 20-25°C. Fluorescence was measured using a fluorescence plate

253 reader with an excitation wavelength of 350 nm and an emission of 600 nm. The increase in  
254 fluorescence intensity yielded the ROS quantity compared to control.

255 Exposed and not exposed daphnids were homogenized in 1 mL sucrose buffer (0.25 M sucrose, 0.1  
256 M Tris-HCl, 1 mM EDTA, pH 7.4) and successively centrifuged at 12.000 g for 15 min at 4°C.

257 Supernatants were collected and used to determinate enzymatic activities. Protein content of the  
258 samples was quantified using the protocol described by Bradford (1976) using bovine serum  
259 albumin as standard.

260 CAT activity was expressed as H<sub>2</sub>O<sub>2</sub> consumed (U·mg<sup>-1</sup> of protein) to convert it to H<sub>2</sub>O and O<sub>2</sub> per  
261 minute, per mg protein at 240 nm (Aebi, 1984).

262 SOD activity was calculated by measuring the decrease in the color development of samples at 440  
263 nm with the reference to the xantine oxidase/cithochrome method (Crapo et al., 1978). In particular  
264 the superoxide radical, generated from the conversion of xanthine to uric acid and H<sub>2</sub>O<sub>2</sub> by xanthine  
265 oxidase, reacts with the tetrazolium salt WST-1 forming formazan.

266 One unit of SOD was defined as the amount of enzyme required to produce 50% inhibition in the  
267 reaction system.

268 GST was calculated by measuring the changes in absorbance recorded at 340 nm due to the  
269 conjugation of glutathione to 1-chloro-2,4-dinitrobenzene (Habig et al., 1974).

270 One unit of enzyme was the quantity necessary for the reduction of 1 μmol·L<sup>-1</sup> GSH in 1 min at 37  
271 °C.

272 Test runs were performed in triplicate with additional controls including on aqueous solutions  
273 containing hydrogen peroxide supplemented with catalase, used to destroy the residual hydrogen  
274 peroxide.

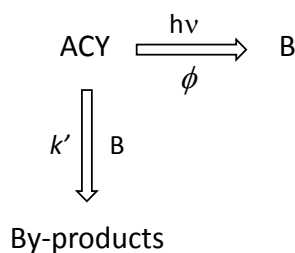
275

## 276 **4. Results and discussion**

### 277 *4.1. UV<sub>254</sub> photolysis: kinetic investigation*



278 The results collected from runs of UV<sub>254</sub> photolysis of ACY in aqueous solution at three different  
 279 pH values (4.5, 6.0 and 8.0) in the MCF photoreactor at varying lamp power are reported in Figs.  
 280 1a-e as a function of the space time. The results indicate that, for a fixed lamp power, the pH did not  
 281 affect the conversion. In fact, for these runs a half-time of about 17 seconds was recorded  
 282 independent of the pH. Moreover, the analysis of the concentration vs time profile demonstrated  
 283 that the photolysis of ACY resembled an apparent autocatalytic behavior which suggested the  
 284 adoption of an autocatalytic kinetic model to describe the degradation of ACY under the adopted  
 285 experimental conditions. Since the destruction of guanine based substrates under UV<sub>254</sub> irradiation  
 286 has been ascribed to both the direct photolysis of guanine derivatives and the reaction of guanine  
 287 based molecules with the radical species formed during the photolytic process (Crespo-Hernandez  
 288 et al., 2000a,b), the simplified reaction scheme (Scheme 1) was considered for the UV<sub>254</sub> photolysis  
 289 of ACY, which is a guanine derivative:



290

291

Scheme 1

292

293 where B indicates a pseudo intermediate (hydrated electron, oxygen reactive species, etc.) capable  
 294 of reacting with ACY molecules according to a simple autocatalytic-type kinetics. The quantum  
 295 yield of photolysis of ACY at 254 nm ( $\phi_{ACY}$ ) and the kinetic constant  $k'$  were estimated through an  
 296 iterative method, using simultaneously the concentration data reported in Figures 1a,e to solve ODE  
 297 equations 1 and 2:

$$\frac{d[\text{ACY}]}{dt} = -P_o \cdot \phi_{\text{ACY}} \cdot (1 - \exp(-2.3 \cdot l_{\text{MCF}} \cdot \epsilon_{254}^{\text{ACY}} \cdot [\text{ACY}])) - k' \cdot [\text{ACY}] \cdot [\text{B}] \quad (1)$$

$$\frac{d[B]}{dt} = P_o \cdot \phi_{ACY} \cdot (1 - \exp(-2.3 \cdot l_{MCF} \cdot \varepsilon_{254}^{ACY} \cdot [ACY])) \quad (2)$$

298 Where  $t$  is the space time in the continuous flow MCF photoreactor (the reaction or exposure time)  
 299 and the term  $\varepsilon_{254}^{ACY}$  is the molar absorption coefficient at 254 nm for ACY at pH 4.5, 6.0 and 8.0  
 300 ( $1.21 \cdot 10^{-2} \text{ M}^{-1} \cdot \text{cm}^{-1}$ ). This result is in agreement with the pKa values of ACY (2.27 and 9.25)  
 301 (Florence, 2010).

302 The MATLAB routine “ode45”, based on the Runge-Kutta method with adaptive step-size, was  
 303 used for the optimization procedure which minimized the objective function  $\sum_j^m \sum_i^n (y_{ACY_{j,i}} -$   
 304  $c_{ACY_{j,i}})^2$ , made by the squares of the differences between the calculated “ $y$ ” and experimental “ $c$ ”  
 305 concentrations of ACY, varying the reaction time “ $n$ ” and for different experimental photolytic runs  
 306 “ $m$ ”. The determined kinetic parameters that minimized the objective function were  $\phi_{ACY} = (1.62 \pm$   
 307  $0.07) \cdot 10^{-3} \text{ mol} \cdot \text{ein}^{-1}$  and  $k' = (5.64 \pm 0.03) \cdot 10^{-3} \text{ M}^{-1} \cdot \text{s}^{-1}$ . The comparison between experimental and  
 308 calculated data, reported in Figures 1a-e including the percentage standard deviations, demonstrated  
 309 close prediction of the concentration profiles of ACY in the MCF photoreactor.

310 The  $\phi_{ACY}$  value reported above has the same order of magnitude as the quantum yield of  
 311 photodecomposition of other guanine derivatives, such as guanosine and 9-ethyl-guanine at similar  
 312 concentrations (Crespo-Hernandez et al., 2000a), thus suggesting that the purine structure could  
 313 play a fundamental role in the UV photolysis of guanine derivatives. The differences could be  
 314 ascribed to a slight effect of the nature of the group attached to the 9-N on the UV-photolysis  
 315 kinetics.

316

#### 317 4.2. $UV_{254}/H_2O_2$ oxidation: kinetic investigation

318 The results of a preliminary run carried out in the presence of hydrogen peroxide under darkness  
 319 indicated that ACY was not degraded in the presence of  $H_2O_2$  alone for reaction times up to 30 min.  
 320 Photooxidation experiments of ACY by the  $UV_{254}/H_2O_2$  process were carried out under the same

321 experimental conditions (i.e., pH, lamp power and initial concentration of ACY) used in the UV<sub>254</sub>  
322 direct photolysis runs.

323 The degradation profiles for ACY and H<sub>2</sub>O<sub>2</sub> as a function of space time in the MCF photoreactor  
324 were modeled on the basis of a simplified reaction scheme and the mass balances listed in Table 2.

325 The reaction scheme considers the consumption of ACY and hydrogen peroxide by direct  
326 photolysis (*reactions 3 and 4*). Hydroxyl radicals generated by UV<sub>254</sub> photolysis of H<sub>2</sub>O<sub>2</sub> can react  
327 with hydrogen peroxide (*reaction 5*), ACY (*reaction 6*) and the transformation products (*reaction*  
328 *7*). A radical termination of peroxy radicals was considered in the mechanism (*reaction 8*).

329 The literature reports two different values of the the kinetic constant of the reaction between  
330 hydroxyl radical and ACY ( $k_{OH/ACY}$ ):  $5.0 \cdot 10^9 \text{ M}^{-1} \cdot \text{s}^{-1}$  (pH=9, T=18 °C, solar simulator  $\lambda > 320 \text{ nm}$ )  
331 (Prasse et al., 2015) and  $1.19 \cdot 10^{10} \text{ M}^{-1} \cdot \text{s}^{-1}$  (pH= 6-9, lamp  $\lambda > 340 \text{ nm}$ ) (Zhou et al., 2015) which  
332 were determined with competition kinetics in the presence of a reference compound (i.e.,  
333 acetophenone, Zhou et al., 2015, and p-chloro-benzoic acid, Prasse et al., 2015). Since these  $k_{OH/ACY}$   
334 values differed by more than 50%,  $k_{OH/ACY}$  was determined using both numerical optimization and  
335 competition kinetics.

336 Specifically, the same iterative optimization procedure reported in section 4.1, using simultaneously  
337 a set of 9 photodegradation runs in distilled water, at different initial concentrations of ACY and  
338 hydrogen peroxide, pH and lamp power, was used for the estimation of  $k_{OH/ACY}$ . The iterative  
339 method minimized the objective function (Eq. 14) that in this case was slightly modified to include  
340 the number of the reacting species ( $h$ ):

$$\Phi = \sum_g^h \sum_j^m \sum_i^n (y_{g,j,i} - c_{g,j,i})^2 \quad (14)$$

341 From this method  $k_{OH/ACY}$  was determined as  $(1.23 \pm 0.07) \cdot 10^9 \text{ M}^{-1} \cdot \text{s}^{-1}$ . Graphical examples of the  
342 results obtained by the modeling through the optimization procedure are shown in Figures 2a-f  
343 (*optimization procedure*). In Figures 2g-i the comparison is reported between experimental and

344 calculated residual ACY and H<sub>2</sub>O<sub>2</sub> concentration, when the model was used in simulation mode  
345 without any further parameter adjustment (*simulation mode*), using the  $k_{OH/ACY}$  kinetic constant  
346 above estimated. It can be noted a good capability of the model of predicting the experimental data  
347 under the adopted conditions.

348 Two additional UV<sub>254</sub>/H<sub>2</sub>O<sub>2</sub> runs (Figs. 2l-m) were carried out using synthetic wastewater to further  
349 validate the kinetic results obtained. The photolytic runs were simulated using the proposed kinetic  
350 model properly modified to include the HO radical scavenging effect of the species forming the  
351 synthetic matrix (Spasiano et al., 2016). For this purpose, the pseudo-first order rate constant ( $k'_{sca} =$   
352  $4.01 \cdot 10^{-1} \text{ s}^{-1}$ ) was considered for the reaction between the hydroxyl radicals and the scavenger  
353 species (Spasiano et al., 2016). Also in this case, a good capability of the model was still observed  
354 to predict the experimental data under the adopted conditions.

355 The competition kinetic method was used to estimate the  $k_{OH/ACY}$  constant in the same MCF  
356 photoreactor, to further validate the kinetic model proposed above. The method compares the ACY  
357 concentration decay to that of benzoic acid (BA) (initial concentration  $2.0 \cdot 10^{-5} \text{ M}$ ) chosen as  
358 reference compound (Onstein et al., 1999):

$$\ln\left(\frac{[ACY]}{[ACY]_0}\right) = \frac{k_{OH/ACY}}{k_{OH/BA}} \cdot \ln\left(\frac{[BA]}{[BA]_0}\right) \quad k_{OH/BA} = 5.9 \cdot 10^9 \text{ M}^{-1} \cdot \text{s}^{-1} \quad (\text{pH} = 6.0) \quad (15)$$

359 An average value  $k_{OH/ACY} = (2.30 \pm 0.11) \cdot 10^9 \text{ M}^{-1} \cdot \text{s}^{-1}$  was thus calculated from UV<sub>254</sub>/H<sub>2</sub>O<sub>2</sub>  
360 experiments carried out at pH = 6.0 and  $[H_2O_2]_0/[ACY]_0 = 20$  and at different lamp power (4.5 W  
361 and 8.0 W). The difference of this from the value estimated with kinetic modeling may be ascribed  
362 to the intrinsic limitations of the competition kinetics method that does not include the contribution  
363 of ACY consumption by direct photolysis. However, both  $k_{OH/ACY}$  values estimated in the present  
364 investigation were significantly lower than those previously reported in the literature (Zhou et al.,  
365 2015; Prasse et al., 2015).

366

367 *4.3. UV<sub>254</sub> photolysis and UV<sub>254</sub>/H<sub>2</sub>O<sub>2</sub> oxidation: Ecotoxicity assessment*

368 A battery of ecotoxicity tests on *V. fischeri*, *D. magna* and *R. subcapitata* were performed on  
369 untreated and treated aqueous solutions with an initial ACY concentration of  $1.2 \text{ mg}\cdot\text{L}^{-1}$ . The  
370 results showed that the inhibition of *V. fischeri* luminescence remained unchanged in the presence  
371 of the  $\text{UV}_{254}$  and  $\text{UV}_{254}/\text{H}_2\text{O}_2$  irradiated solutions, in comparison to the untreated solution (data not  
372 shown).

373 The results obtained for *D. magna* (exposure time = 24 and 48 h) for the  $\text{UV}_{254}$  and  $\text{UV}_{254}/\text{H}_2\text{O}_2$   
374 treated and untreated samples are reported in Figures 3A,B. The samples treated with  $\text{UV}_{254}$   
375 irradiation in the absence of hydrogen peroxide, initially showed an increase of immobility of  
376 daphnids at increasing  $\text{UV}_{254}$  dose and consequently at higher ACY conversion, suggesting an  
377 increase in acute ecotoxicity, although, this eventually decreased significantly at the highest  $\text{UV}_{254}$   
378 dose. On the other hand, the acute ecotoxicity of the  $\text{UV}_{254}/\text{H}_2\text{O}_2$  treated solutions toward *D. magna*  
379 was significantly lower in comparison to the samples treated with  $\text{UV}_{254}$  only, even at much lower  
380 UV doses. It is important to note that the acute ecotoxicity of the  $\text{UV}_{254}$  sample after complete  
381 conversion of ACY was higher than the value for the un-irradiated control sample.

382 The inhibition growth of *R. subcapitata* reached 32%, 13% and 20% at  $\text{UV}_{254}$  doses of 864, 2356  
383 and  $4712 \text{ mJ}\cdot\text{cm}^{-2}$  respectively (Fig. 4), thus confirming an acute toxicological effect on the  $\text{UV}_{254}$   
384 only treated samples. In contrast, a small reduction of the inhibition growth was observed for the  
385 samples treated with  $\text{UV}_{254}/\text{H}_2\text{O}_2$  at increasing  $\text{UV}_{254}$  doses, which supported the beneficial effect  
386 of the  $\text{H}_2\text{O}_2$  assisted photolytic treatment for toxicity reduction.

387 The results showed an increase of the production of ROS in all samples, that could enhance the  
388 sublethal toxicity in daphnids. Aquatic organisms can in fact adapt to an increase of ROS  
389 production by upregulating the activity of their antioxidant enzymes, particularly of CAT and SOD  
390 which represent the first and the second line of defense against ROS (Oexle et al., 2016). An  
391 evident increase of ROS production in the daphnids treated with  $\text{UV}_{254}$  only samples was observed  
392 in comparison to the those treated with the  $\text{UV}_{254}/\text{H}_2\text{O}_2$  samples (Fig. 5A). The increase was

393 recorded for UVC doses of 864 and 2356  $\text{mJ}\cdot\text{cm}^{-2}$  for the  $\text{UV}_{254}$  process and at 280  $\text{mJ}\cdot\text{cm}^{-2}$  for the  
394 samples treated with  $\text{UV}_{254}/\text{H}_2\text{O}_2$ .

395 The SOD activity resulted in significant alterations only for samples treated by  $\text{UV}_{254}$  (Fig. 5B).

396 The enzyme inhibition increased when the UVC dose was increased and reached the highest  
397 inhibition at 2356  $\text{mJ}\cdot\text{cm}^{-2}$ . No effect was observed in the samples treated with  $\text{UV}_{254}/\text{H}_2\text{O}_2$  except  
398 for samples treated with a UVC dose of 280  $\text{mJ}\cdot\text{cm}^{-2}$  (TOC removal degree: 28%).

399 Both processes led to a significant increase of CAT activity compared to the control (Fig. 5C), since  
400 CAT is responsible for the detoxification of high levels of hydrogen peroxide, one of the most  
401 important ROS producers under oxidative stress conditions.

402 On the contrary, GST activity remained unchanged or decreased with both treatments as shown in  
403 Figure 5D. Probably the response patterns may be species-specific in nature, while varying in  
404 intensity response. The antioxidant enzymes can maintain cellular redox balance, alleviate the  
405 toxicological effects of ROS and protect the cells against the oxidative damage of their structures  
406 including lipid, membranes, proteins and nucleic acids (Oropesa et al., 2017).

407 A 21 days chronic exposure experiment was performed to determine the toxicity of 100 fold diluted  
408 untreated and treated solutions. The effects of ACY (120  $\mu\text{g}\cdot\text{L}^{-1}$ ) and its treated samples on *D.*  
409 *magna* reproduction and survival are reported in Figure 6A,B.

410 The results of chronic toxicity showed that the  $\text{UV}_{254}$  treatment, even at such low concentrations of  
411 ACY, significantly decreased the survival of *D. magna* compared to the control group. A decrease  
412 of survival was further recorded for samples exposed at a TOC removal of less than 5% (ACY  
413 conversion degree: 45%), probably due the presence of unconverted ACY, and at  $\text{UV}_{254}$  dose of  
414 2356  $\text{mJ}\cdot\text{cm}^{-2}$  (ACY conversion: 90%), due to the formation of first-generation-transformation by-  
415 products structurally similar to ACY. At higher  $\text{UV}_{254}$  doses (4712  $\text{mJ}\cdot\text{cm}^{-2}$ , TOC removal  $\sim$  5%),  
416 the survival percentage was similar to that of the control samples and always higher to that of the  
417 untreated sample. On the contrary, the ecotoxicity assessment for the  $\text{UV}_{254}/\text{H}_2\text{O}_2$  treated solutions

418 reflected the results already recorded in the acute tests, revealing a marked reduction of chronic  
419 toxic effects for the exposures of the daphnids to the UV<sub>254</sub>/H<sub>2</sub>O<sub>2</sub> samples, especially the highest  
420 UV<sub>254</sub> doses (950 mJ·cm<sup>-2</sup>, TOC removal 77% and 1900 mJ·cm<sup>-2</sup>, TOC removal higher than 95%).  
421 As reported in Table 3, the reproduction of *D. magna* was completely inhibited in the organisms  
422 contacted with samples exposed to UV<sub>254</sub> doses of 864 mJ·cm<sup>-2</sup> and 2356 and in absence of H<sub>2</sub>O<sub>2</sub>.  
423 These results revealed that all the endpoints were different than the control solutions with an  
424 extended exposure to the treatment, thus confirming that the photoproducts formed during UV<sub>254</sub>  
425 irradiation of aqueous ACY solutions exerted significant chronic adverse effects to *D. magna* at the  
426 population level. On the contrary, the total number of neonates and the number of first-brood were  
427 not statistically different among the samples untreated and treated by UV<sub>254</sub>/H<sub>2</sub>O<sub>2</sub>.  
428 The different chemical species formed during the UV<sub>254</sub> and the UV<sub>254</sub>/H<sub>2</sub>O<sub>2</sub> photochemical  
429 processes could reasonably explain the observed toxicological effects. To provide a preliminary  
430 validation of this hypothesis, two samples, one from UV<sub>254</sub> photolysis and the second from  
431 UV<sub>254</sub>/H<sub>2</sub>O<sub>2</sub> treatment, were directly analyzed with MS-spectrometer to identify the main chemical  
432 intermediates formed, with the knowledge that a thorough identification of the transformation by-  
433 products required more sophisticated diagnostic techniques (Buchberger, 2011).  
434 A list of molecular structures of the main intermediates that could be attributed to some peaks  
435 detected in the mass spectra for two samples is reported in Table 4. Some of the structures shown in  
436 Table 4 correspond to the chemical intermediates previously detected and reported in literature. In  
437 particular, for the UV<sub>254</sub> photolysis, the structures II, IV and V were observed during the  
438 degradation of ACY by TiO<sub>2</sub> photocatalysis at 365 nm (An et al., 2015) whereas the by-products  
439 VII and X proposed for UV<sub>254</sub>/H<sub>2</sub>O<sub>2</sub> were the same of those observed during the photooxidation of  
440 ACY in phosphate buffer at wavelength higher than 270 nm (Iqbal et al., 2005).. The attribution of  
441 reliable structures to the remaining recorded MS signals not previously observed by others, needs  
442 further analytical assessments. However, although an uncomplete analysis is available for the  
443 products of degradation of ACY, the data collected indicated the presence of chemical species

444 significantly different in the two samples. In particular, UV<sub>254</sub>/H<sub>2</sub>O<sub>2</sub> process seems to lead mainly to  
445 the formation of hydroxylated imidazole-based compounds or species formed by the fragmentation  
446 of the pyrimidine ring whereas some hydroxylated ACY based intermediates are detected in the  
447 UV<sub>254</sub> treated sample.

448

## 449 **5. Conclusion**

450 The photodegradation of ACY was investigated under UV<sub>254</sub> irradiation in the absence and in the  
451 presence of hydrogen peroxide. A moderate rate of direct photolysis at 254 nm for ACY was  
452 observed with a quantum yield of  $(1.62 \pm 0.073) \cdot 10^{-3} \text{ mol} \cdot \text{ein}^{-1}$  in the pH range 4.5 – 8.0. An  
453 average value of  $1.76 \cdot 10^9 \text{ M}^{-1} \cdot \text{s}^{-1}$  was calculated for the kinetic constant of reaction between  
454 hydroxyl radical and ACY. Considering (i) the UV<sub>254</sub> doses typically used for the disinfection of  
455 municipal sewage treatment plant effluents, (ii) the concentration values of ACY measured in  
456 WWTP effluents, and (iii) the results collected during the kinetic and ecotoxicity assessment, the  
457 occurrence of residual photodecomposition by-products in treated effluents is very likely, and these  
458 are likely to have a high ecotoxicological index. However, the addition of appropriate amount of  
459 hydrogen peroxide during the UV<sub>254</sub> disinfection stage would reduce this risk.

460 The results obtained contribute to provide useful information for a vision about the fate of ACY  
461 during the UV<sub>254</sub> and UV<sub>254</sub>/H<sub>2</sub>O<sub>2</sub> treatment processes and the eventual associated risks for living  
462 organisms (animals and plants) in the aquatic environment.

463 The results collected confirm the use of oxidative stress biomarkers as promising tool in order to  
464 evaluate the toxicological effects of environmental pollutants as early indicators in ecotoxicology.  
465 Exposure to environmental pollutants may disrupt the balance of biological oxidant-to-antioxidant  
466 ratio in aquatic species leading to elevated levels of ROS and resulting in oxidative stress. A  
467 preliminary analysis on the treated samples indicated, as the main photo-transformation by-  
468 products, the presence of hydroxylated ACY based intermediates in the UV<sub>254</sub> treatment process,



469 and hydroxylated imidazole based compounds or species formed by the fragmentation of the  
470 pyrimidine ring in the UV<sub>254</sub>/H<sub>2</sub>O<sub>2</sub> treatment process.

471 Further efforts are required to identify the main photoproducts, to elucidate the mechanism of ACY  
472 photodegradation under UVC radiation and to evaluate possible cumulative effects of the different  
473 species occurring in STP effluents.

474

#### 475 **Acknowledgements**

476 The Authors are grateful to ERASMUS-Mobility Student Program, and to Ing. Giulio Di Costanzo  
477 for his precious support during the experimental campaign.

478

#### 479 **References**

480 Aebi, H., (1984) Catalase in vitro. *Methods in Enzymology* 6, 105–121.

481 An, T., An, J., Gao, Y., Li, G., Fang, H., Song, W. (2015) Photocatalytic degradation and  
482 mineralization mechanism and toxicity assessment of antiviral drug acyclovir: Experimental and  
483 theoretical studies. *Applied Catalysis B: Environmental* 164, 279–287.

484 Asano, T. (1998) *Wastewater Reclamation and Reuse*, in *Water Quality Management Library*, Vol  
485 10. C.R.C. Press, Boca Raton.

486 Azuma, T., Arima, N., Tsukada, A., Hirami, S., Matsuoka, R., Moriwake, R., Ishiuchi, H., Inoyama,  
487 T., Teranishi, Y., Yamaoka, M., Mino, Y., Hayashi, T., Fujita, Y., Masada, M. (2016) Detection of  
488 pharmaceuticals and phytochemicals together with their metabolites in hospital effluents in Japan,  
489 and their contribution to sewage treatment plant influents. *Science of the Total Environment* 548–  
490 549, 189–197.

491 Bielski, B.H., Cabelli, D.E., Aruda, R.L., Ross, A.B. (1985) Reactivity of HO<sub>2</sub>/O<sub>2</sub> radicals in  
492 aqueous solution. *Journal of Physical and Chemical Reference Data* 14, 1041-1077.

493 Bradford, M.M. (1976) A rapid and sensitive method for the quantitation of microgram quantities of  
494 protein utilizing the principle of protein-dye binding. *Anal. Biochem.* 72, 248–254.

495 Bradley, P.M., Barber, L.B., Duris, J.W., Foreman, W.T., Furlong, E.T., Hubbard, L.E.,  
496 Hutchinson, K.J., Keefe, S.H., Kolpin, D.W. (2014) Riverbank filtration potential of  
497 pharmaceuticals in a wastewater-impacted stream. *Environmental Pollution* 193, 173–180.

498 Bryan-Marrugo, O.L., Ramos-Jiménez, J., Barrera-Saldana, H., Rojas-Martínez, A., Vidaltamayo,  
499 R., Rivas-Estilla, A.M. (2015) History and progress of antiviral drugs: From acyclovir to direct-  
500 acting antiviral agents (DAAs) for Hepatitis C. *Medicina Universitaria* 17(68), 165–174.

501 Buchberger, W.W. (2011) Current approaches to trace analysis of pharmaceuticals and personal  
502 care products in the environment. *Journal of Chromatography A* 1218, 603–618.

503 Buxton, G.V., Greenstock, C.L., Helman, W.P., Ross, A.B. (1988) Critical review of rate constants  
504 for reactions of hydrated electrons, hydrogen atoms and hydroxyl radicals (OH/O) in aqueous  
505 solution. *Journal of Physical and Chemical Reference Data* 17, 513–886.

506 Canonica, S., Meunier, L., von Gunten, U. (2008) Phototransformation of selected pharmaceuticals  
507 during UV treatment of drinking water. *Water Research* 42, 121–128.

508 Conner-Kerr, T.A., Sullivan, P.K., Gaillard, J., Franklin, M.E., Jones, R.M. (1998) The effects of  
509 ultraviolet radiation on antibiotic-resistant bacteria in vitro. *Ostomy Wound Manage.* 44, 50–56.

510 Crapo, J.D., McCord, J.M., Fridovich, I. (1978) Preparation and assay of superoxide dismutases.  
511 *Methods in Enzymology* 53, 382–393.

512 Crespo-Hernandez, C.E., Flores, S., Torres, C., Negron-Encarnacion, I., Arce, R. (2000a) Part I.  
513 Photochemical and photophysical studies of guanine derivatives: intermediates contributing to its  
514 photodestruction mechanism in aqueous solution and the participation of the electron adduct.  
515 *Photochemistry and Photobiology* 71(5), 534–543.

516 Crespo-Hernandez, C.E., Arce, R. (2000b) Part II. Mechanism of formation of guanine as one of the  
517 major products in the 254 nm photolysis of guanine derivatives: concentration and pH effects.  
518 *Photochemistry and Photobiology* 71(5), 544–550.

519 Da Silva, L.M., Cavalcante, R.P., Cunha, R.F., Gozzi, F., Dantas, R.F., De Oliveira, S.C.,  
520 Machulek, A.J. (2016) Tolfenamic acid degradation by direct photolysis and the UV-ABC/H<sub>2</sub>O<sub>2</sub>

521 process: factorial design, kinetics, identification of intermediates, and toxicity evaluation. *Science*  
522 *of the Total Environment* 573, 518–531.

523 DVGW, 1997. W 294. UV-Desinfektionsanlagen für die Trinkwasserversorgung-Anforderungen  
524 und Prüfung.

525 FDA (Food and Drug Administration). Guidance for Industry: Environmental Assessment of  
526 Human Drug and Biologics Application. CDER/CBER CMC 6, rev 1, 39 pp, July 1998. Available:  
527 <http://www.fda.gov/cber/guidelines.htm>.

528 Florence, A. T. (2010) *An Introduction to Clinical Pharmaceutics*. Ed. Pharmaceutical Press,  
529 London.

530 Funke, J., Prasse, C., Ternes, T.A. (2016) Identification of transformation products of antiviral  
531 drugs formed during biological wastewater treatment and their occurrence in the urban water cycle.  
532 *Water Research* 98, 75–83.

533 Galdiero, E., Siciliano, A., Maselli, V., Gesuele, R., Guida, M., Fulgione, D., Galdiero, S.,  
534 Lombardi, L., Falanga, A. (2016) An integrated study on antimicrobial activity and ecotoxicity of  
535 quantum dots and quantum dots coated with the antimicrobial peptide indolicidin. *International*  
536 *Journal of Nanomedicine* 11, 4199–4211.

537 García-Galan, M. J., Anfruns, A., Gonzalez-Olmos, R., Rodriguez-Mozaz, S., Comas, J. (2016)  
538 Advanced oxidation of the antibiotic sulfapyridine by UV/H<sub>2</sub>O<sub>2</sub>: Characterization of its  
539 transformation products and ecotoxicological implications. *Chemosphere* 147, 451–459.

540 Gillman, A., Nykvist, M., Muradrasoli, S., Soderstrom, H., Wille, M., Daggfeldt, A., Brojer, C.,  
541 Waldenstrom, J., Olsen, B., Jarhult, J.D. (2015) Influenza A(H7N9) virus acquires resistance-  
542 related neuraminidase I222T substitution when infected mallards are exposed to low levels of  
543 oseltamivir in water. *Antimicrobial Agents and Chemotherapy* 59(9), 5196–5202.

544 Goldstein, S., Aschengrau, D., Diamant, Y., Rabani, J. (2007) Photolysis of aqueous H<sub>2</sub>O<sub>2</sub>:  
545 quantum yield and applications for polychromatic UV actinometry in photoreactors. *Environmental*  
546 *Science & Technology* 41, 7486-7490.

547 Guo, M.T., Yuan, Q.B., Yang, J. (2013) Ultraviolet reduction of erythromycin and  
548 tetracyclineresistant heterotrophic bacteria and their resistance genes in municipal wastewater.  
549 Chemosphere 93, 2864–2868.

550 Habig, W.H., Pabst, M.J., Jakoby, W.B. (1974) Glutathione-S-transferases. The first step in  
551 mercapturic acid formation. Journal of Biological Chemistry 249, 7130–7139.

552 Hijnen, W.A.M., Beerendonk, E.F., Medema, G.J. (2006) Inactivation credit of UV radiation for  
553 viruses, bacteria and protozoan (oo)cysts in water: a review. Water Research 40 (1), 3–22.

554 Hill, A., Khoo, S., Fortunak, J., Simmons, B., Ford, N. (2014) Minimum costs for producing  
555 hepatitis C direct-acting antivirals for use in large-scale treatment access. Programs in Developing  
556 Countries. Clinical Infectious Diseases 58(7), 928–936.

557 Hoekstra, A.Y. (2014) Water scarcity challenges to business. Nature Climate Change 4, 318–322.

558 Huang, J.J., Hu, H.Y., Tang, F., Li, Y., Lu, S.Q. Lu, Y. (2011) Inactivation and reactivation of  
559 antibiotic-resistant bacteria by chlorination in secondary effluents of a municipal wastewater  
560 treatment plant. Water Research 45, 2775–2781.

561 Iqbal, J., Husain, A., Gupta, A. (2005) Photooxidation of acyclovir in aqueous solution. Pharmazie  
562 60(8), 574–576

563 ISO 6341:2013 Water quality: determination of the inhibition of the mobility of *Daphnia magna*  
564 Straus (Cladocera, Crustacea) acute toxicity test.

565 ISO 8692:2012 Water quality: fresh water algal growth inhibition test with unicellular green algae.

566 ISO 11348-3:2007 Water quality: determination of the inhibitory effect of water samples on the  
567 light emission of *Vibrio fischeri* (Luminescent bacteria test), part 3: method using freeze-dried  
568 bacteria.

569 Jain, S., Kumar, P., Vyas, R.K., Pandit, P., Dalai, A.K. (2013) Occurrence and removal of antiviral  
570 drugs in environment: A review. Water, Air, & Soil Pollution 224, 1410–1419.

571 Khan, S., Beattie, T.K., Knapp, C.W. (2016) Relationship between antibiotic- and disinfectant-  
572 resistance profiles in bacteria harvested from tap water. Chemosphere 152, 132–141.

573 Kim, I., Yamashita, N., Tanaka, H. (2009) Photodegradation of pharmaceuticals and personal care  
574 products during UV and UV/H<sub>2</sub>O<sub>2</sub> treatments. *Chemosphere* 77, 518–525.

575 Kovacic, M., Perisic, D.J., Biosic, M., Kusic, H., Babic, S., Bozic, A.L. (2016) UV photolysis of  
576 diclofenac in water; kinetics, degradation pathway and environmental aspects. *Environmental*  
577 *Science and Pollution Research* 23, 14908–14917.

578 Liu, W.R., Ying, G.G., Zhao, J.L., Liu, Y.S., Hu, L.X., Yao, L., Liang, Y.Q., Tian, F. (2016)  
579 Photodegradation of the azole fungicide climbazole by ultraviolet irradiation under different  
580 conditions: Kinetics, mechanism and toxicity evaluation. *Journal of Hazardous Materials* 318, 794–  
581 801.

582 Lofrano, G., Libralato, G., Adinolfi, R., Siciliano, A., Iannece, P., Guida, M., Giugni, M., Volpi  
583 Ghirardini, A., Carotenuto, M. (2016) Photocatalytic degradation of the antibiotic chloramphenicol  
584 and its by-products toxicity effects. *Ecotoxicology and Environmental Safety* 123, 65–71.

585 Ma, J., Lv, W., Chen, P., Lu, Y., Wang, F., Li, F., Yao, K., Liu, G. (2016) Photodegradation of  
586 gemfibrozil in aqueous solution under UV irradiation: kinetics, mechanism, toxicity, and  
587 degradation pathways. *Environmental Science and Pollution Research* 23, 14294–14306.

588 Marotta, R., Spasiano, D., Di Somma, I., Andreozzi, R. (2013) Photodegradation of naproxen and  
589 its photoproducts in aqueous solution at 254 nm: a kinetic investigation. *Water Research* 47, 373–  
590 383.

591 McCurry, D.L., Bear, S.E., Bae, J., Sedlak, D.L., McCarty, P.L., Mitch, W.A. (2014) Superior  
592 removal of disinfection byproduct precursors and pharmaceuticals from wastewater in a staged  
593 anaerobic fluidized membrane bioreactor compared to activated sludge. *Environmental Science &*  
594 *Technology Letters* 1, 459–464.

595 Meckes, M.C. (1982) Effect of UV light disinfection on antibiotic-resistant coliforms in wastewater  
596 effluents. *Appl. Environ. Microbiol.* 43, 371–377.

597 Montemayor, M., Costan, A., Lucena, F., Jofre, J., Munoz, J., Dalmau, E., Mujeriego, R., Salas L.  
598 (2008) The combined performance of UV light and chlorine during reclaimed water disinfection.  
599 Water Science & Technology 57(6), 935–940.

600 Munir, M., Wong, K., Xagorarakis, I. (2011) Release of antibiotic resistant bacteria and genes in the  
601 effluent and biosolids of five wastewater utilities in Michigan. Water Research 45, 681–693.

602 Nick, K., Scholer, H.F., Mark, G., Soylemez, T., Akhlaq, M.S., Schuchmann, H.P., von Sonntag, C.  
603 (1992) Degradation of some triazine herbicides by UV radiation such as used in the UV disinfection  
604 of drinking water. Journal of Water Supply: Research and Technology Aqua 41(2), 82–87

605 Nicole, I., De Laat, J., Doré, M., Duguet, J.P., Bonnel, C. (1990) Use of UV radiation in water  
606 treatment: measurement of photonic flux by hydrogen peroxide actinometry. Water Research 24,  
607 157-168.

608 NWRI (2012) Ultraviolet Disinfection: Guidelines for Drinking Water and Water Reuse, Third  
609 Edition. Published by National Water Research Institute.

610 OECD (2012) Guidelines for Testing of Chemicals. Daphnia magna Reproduction Test. OECD 211.  
611 Paris, France.

612 Oexle, S., Jansen, M., Pauwels, K., Sommaruga, M., De Meester, L., Stoks, R. (2016) Rapid  
613 evolution of antioxidant defence in a natural population of *Daphnia magna*. Journal of Evolutionary  
614 Biology 29, 1328–1337.

615 ONorm, M. (2001). Anlagen zur Desinfektion von Wasser mittels Ultraviolett-Strahlen.  
616 Anforderungen und Prüfung 5873–1.

617 Onstein, P., Stefan, M.I., Bolton, J.R. (1999) Competition kinetics method for the determination of  
618 rate constants for the reaction of hydroxyl radicals with organic pollutants using the UV/H<sub>2</sub>O<sub>2</sub>  
619 advanced oxidation technology: the rate constants for the tert-butylformate ester and 2,4-  
620 dinitrophenol. Journal of Advanced Oxidation Technologies 4(2), 231–236.

621 Organisation for Economic Cooperation and development (OECD), 1999. Guidelines for testing of  
622 chemicals, simulation test-aerobic sewage treatment, 303A.

623 Oropesa, A.L., Novais, S.C., Lemos, M.F.L. Espejo, A., Gravato, C., Beltran, F. (2017) Oxidative  
624 stress response of *Daphnia magna* exposed to effluents spiked with emerging contaminants under  
625 ozonation and advanced oxidation process. *Environmental Science & Pollution Research* 24, 1735–  
626 1747.

627 Peng, X., Wang, C., Zhang, K., Wang, Z., Huang, Q., Yu, Y., Ou, W. (2014) Profile and behavior  
628 of antiviral drugs in aquatic environments of the Pearl River Delta, China. *Science of the Total*  
629 *Environment* 466–467, 755–761.

630 Pereira, V.J., Weinberg, H.S., Linden, K.G., Singer, P.C. (2007) UV degradation of pharmaceutical  
631 compounds in surface water via direct and indirect photolysis at 254 nm. *Environmental Science &*  
632 *Technology* 41(5), 1682–1688.

633 Prasse, C., Schlusener, M.P., Schulz, R., Ternes, T.A. (2010) Antiviral drugs in wastewater and  
634 surface waters: A new pharmaceutical class of environmental relevance? *Environmental Science &*  
635 *Technology* 44, 1728–1735.

636 Prasse, C., Wagner, M., Schulz, R., Ternes, T.A. (2011) Biotransformation of the antiviral drugs  
637 acyclovir and penciclovir in activated sludge treatment. *Environmental Science &*  
638 *Technology* 45(7), 2761–2769.

639 Prasse, C., Wenk, J., Jasper, J.T., Ternes, T.A., Sedlak, D.L. (2015) Co-occurrence of photochemical  
640 and microbiological transformation processes in open-water unit process wetlands. *Environmental*  
641 *Science & Technology* 49, 14136–14145.

642 Reis, N.M., Li Puma, G. (2015) Novel microfluidics approach for extremely fast and efficient  
643 photochemical transformations in fluoropolymer microcapillary films. *Chemical Communications*  
644 51, 8414–8417.

645 Richardson, S.D. (2012) Environmental mass spectrometry: emerging contaminants and current  
646 issues. *Analytical Chemistry* 84, 747–778.

647 Richardson, S.D., Plewa, M.J., Wagner, E.D., Schoeny, R., DeMarini, D.M. (2007) Occurrence,  
648 genotoxicity, and carcinogenicity of regulated and emerging disinfection by-products in drinking  
649 water: a review and roadmap for research. *Mutation Research* 636(1-3), 178-242.

650 Rozas, O., Vidal, C., Baeza, C., Jardim, W.F., Rossner, A., Mansilla, H.D. (2016) Organic  
651 micropollutants (OMPs) in natural waters: Oxidation by UV/H<sub>2</sub>O<sub>2</sub> treatment and toxicity  
652 assessment. *Water Research* 98, 109–118.

653 Russo, D., Spasiano, D., Vaccaro, M., Andreozzi, R., Li Puma, G., Reis, N.M., Marotta, R. (2016)  
654 Direct photolysis of benzoylecgonine under UV irradiation at 254 nm in a continuous flow  
655 microcapillary array photoreactor. *Chemical Engineering Journal* 283, 243–250.

656 Sanderson, H., Johnson, D.J., Reitsma, T., Brain, R.A., Wilson, C.J., Solomon, K.R. (2004)  
657 Ranking and prioritization of environmental risks of pharmaceuticals in surface waters. *Regulatory  
658 Toxicology and Pharmacology* 39(2), 158–183.

659 Shi, P., Jia, S., Zhang, X.X., Zhang, T., Cheng, S., Li, A. (2013) Metagenomic insights into  
660 chlorination effects on microbial antibiotic resistance in drinking water. *Water Research* 47, 111–  
661 120.

662 Singer, A.C., Nunn, M.A., Gould, E.A., Johnson, A.C. (2007) Potential risks associated with the  
663 proposed widespread use of Tamiflu. *Environmental Health Perspectives* 115(1), 102–106.

664 Sinha, V.R., Monika, Trehan, A., Kumar, M., Singh, S., Bhinge, J.R. (2007) Stress studies on  
665 Acyclovir. *Journal of Chromatographic Science* 45, 319–324.

666 Spasiano, D., Russo, D., Vaccaro, M., Siciliano, A., Marotta, R., Guida, M., Reis, N.M., Li Puma,  
667 G., Andreozzi, R. (2016) Removal of benzoylecgonine from water matrices through UV<sub>254</sub>/H<sub>2</sub>O<sub>2</sub>  
668 process: reaction kinetic modeling, ecotoxicity and genotoxicity assessment. *Journal of Hazardous  
669 Materials* 318, 515–525.

670 Yuan, F., Hu, C., Hu, X., Wei, D., Chen, Y., Qu, J. (2011) Photodegradation and toxicity changes  
671 of antibiotics in UV and UV/H<sub>2</sub>O<sub>2</sub> process. *Journal of Hazardous Materials* 185, 1256–1263.



672 Zhou, C., Chen, J., Xie, Q., Wei, X., Zhang, Y., Fu, Z. (2015) Photolysis of three antiviral drugs  
673 acyclovir, zidovudine and lamivudine in surface freshwater and seawater. *Chemosphere* 138, 792–  
674 797.

**Table**[Click here to download Table: Tables revised.docx](#)

WWTP effluent (ng/L)	Surface water (ng/L)	Location	Ref
27.3 – 53.3	2.2 - 190	Germany	(Prasse et al., 2010)
121- 148	5 - 25	Germany	(Prasse et al., 2011)
44.0 - 650	--	Germany	(Funke et al., 2016)
114 - 205	8.9 – 112.6	China	(Peng et al., 2014)
12 - 50	10 - 23	Japan	(Azuma et al., 2016)
947	738 - 1590	USA	(Bradley et al., 2014)
154	--	USA	(McCurry et al., 2014)

Table 1

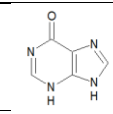
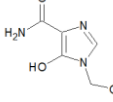
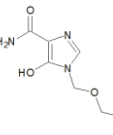
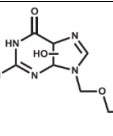
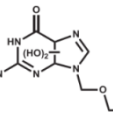
3)	$ACY \xrightarrow{h\nu} \text{TPs}$	$\Phi_{ACY}$	(estimated in this study)
4)	$H_2O_2 \xrightarrow{h\nu} 2HO^\bullet$	$\Phi_{H_2O_2} = 0.55 \text{ mol} \cdot \text{ein}^{-1}$ $\varepsilon_{254}^{H_2O_2} = 18.6 \text{ M}^{-1} \cdot \text{cm}^{-1}$	(Goldstein et al., 2007)
5)	$HO^\bullet + H_2O_2 \xrightarrow{k_h} H_2O + HO_2^\bullet$	$k_h = 2.7 \cdot 10^7 \text{ M}^{-1} \cdot \text{s}^{-1}$	(Buxton et al., 1988)
6)	$ACY + HO^\bullet \xrightarrow{k_{OH/ACY}} \text{TPs}$	$k_{OH/ACY}$	(estimated in this study)
7)	$\text{TPs} + HO^\bullet \xrightarrow{k_{OH/TP}} \text{TP}$	$k_{OH/TP}$	(estimated in this study)
8)	$2HO_2^\bullet \xrightarrow{k_t} H_2O_2 + O_2$	$k_t = 8.3 \cdot 10^5 \text{ M}^{-1} \cdot \text{s}^{-1}$	(Bielski et al., 1985)
9)	$\frac{d[HO^\bullet]}{d\tau} = 2F_{H_2O_2} - [HO^\bullet] \cdot (k_h \cdot [H_2O_2] - k_{OH/ACY} \cdot [ACY] - k_{OH/TP} \cdot [TPs])$		
10)	$F_{H_2O_2} = \Phi_{H_2O_2} \cdot P_o \cdot \left(1 - \exp\left(-2.3 \cdot l_{MCF} \cdot (\varepsilon_{254}^{ACY} \cdot [ACY] + \varepsilon_{254}^{H_2O_2} \cdot [H_2O_2])\right)\right) \cdot f_{H_2O_2}$		
11)	$\frac{d[HO_2^\bullet]}{d\tau} = k_h \cdot [HO^\bullet] \cdot [H_2O_2] - 2k_t \cdot [HO_2^\bullet]^2$		
12)	$\frac{d[ACY]}{d\tau} = -F_{ACY} - k_{OH/ACY} \cdot [ACY] \cdot [HO^\bullet]$		
13)	$F_{ACY} = \Phi_{ACY} \cdot P_o \cdot \left(1 - \exp\left(-2.3 \cdot l_{MCF} \cdot (\varepsilon_{254}^{ACY} \cdot [ACY] + \varepsilon_{254}^{H_2O_2} \cdot [H_2O_2])\right)\right) \cdot f_{ACY}$		

Table 2

<b>UV<sub>254</sub></b>		
Sample	First brood (day)	Number of Living offspring per parent animal
Control solution	8	78 ± 5
UV <sub>254</sub> dose: 0 mJ·cm <sup>-2</sup>	10	72 ± 3
UV <sub>254</sub> dose: 864 mJ·cm <sup>-2</sup> <b>TOC removal degree: &lt; 5%</b>	15	42 ± 3
UV <sub>254</sub> dose: 2356 mJ·cm <sup>-2</sup> <b>TOC removal degree: &lt; 5%</b>	17	37 ± 6
UV <sub>254</sub> dose: 4712 mJ·cm <sup>-2</sup> <b>TOC removal degree: ~ 5%</b>	11	68 ± 5
<b>UV<sub>254</sub>/H<sub>2</sub>O<sub>2</sub></b>		
Sample	First brood (day)	Number of Living offspring per parent animal
Control solution	8	75 ± 1
UV <sub>254</sub> dose: 0 mJ·cm <sup>-2</sup>	10	74 ± 4
UV <sub>254</sub> dose: 280 mJ·cm <sup>-2</sup> <b>TOC removal degree: 28 %</b>	9	69 ± 5
UV <sub>254</sub> dose: 950 mJ·cm <sup>-2</sup> <b>TOC removal degree: 77 %</b>	9	65 ± 2
UV <sub>254</sub> dose: 1900 mJ·cm <sup>-2</sup> <b>TOC removal degree: &gt; 95 %</b>	9	70 ± 2

Table 3

UV<sub>254</sub>

n°	Previously reported	Measured mass [M+H] <sup>+</sup> (Da)	Structure <sup>(c)</sup>
I	NO	136.93	
II	YES, An et al, 2015	158.15	
III	NO	202.18	
IV	YES, An et al, 2015	242.98	
V	YES, An et al, 2015	258.98	

UV<sub>254</sub>/H<sub>2</sub>O<sub>2</sub>

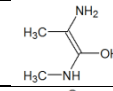
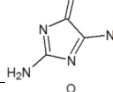
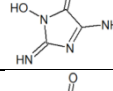
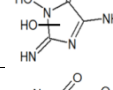
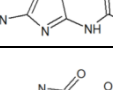
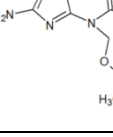
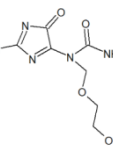
VI	NO	103.08	
VII	YES, Iqbal et al., 2005	113.07	
VIII	NO	129.07	
IX	NO	146.09	
X	YES, Iqbal et al., 2005	156.08	
XI	NO	214.17	
VI	NO	230.12	

Table 4

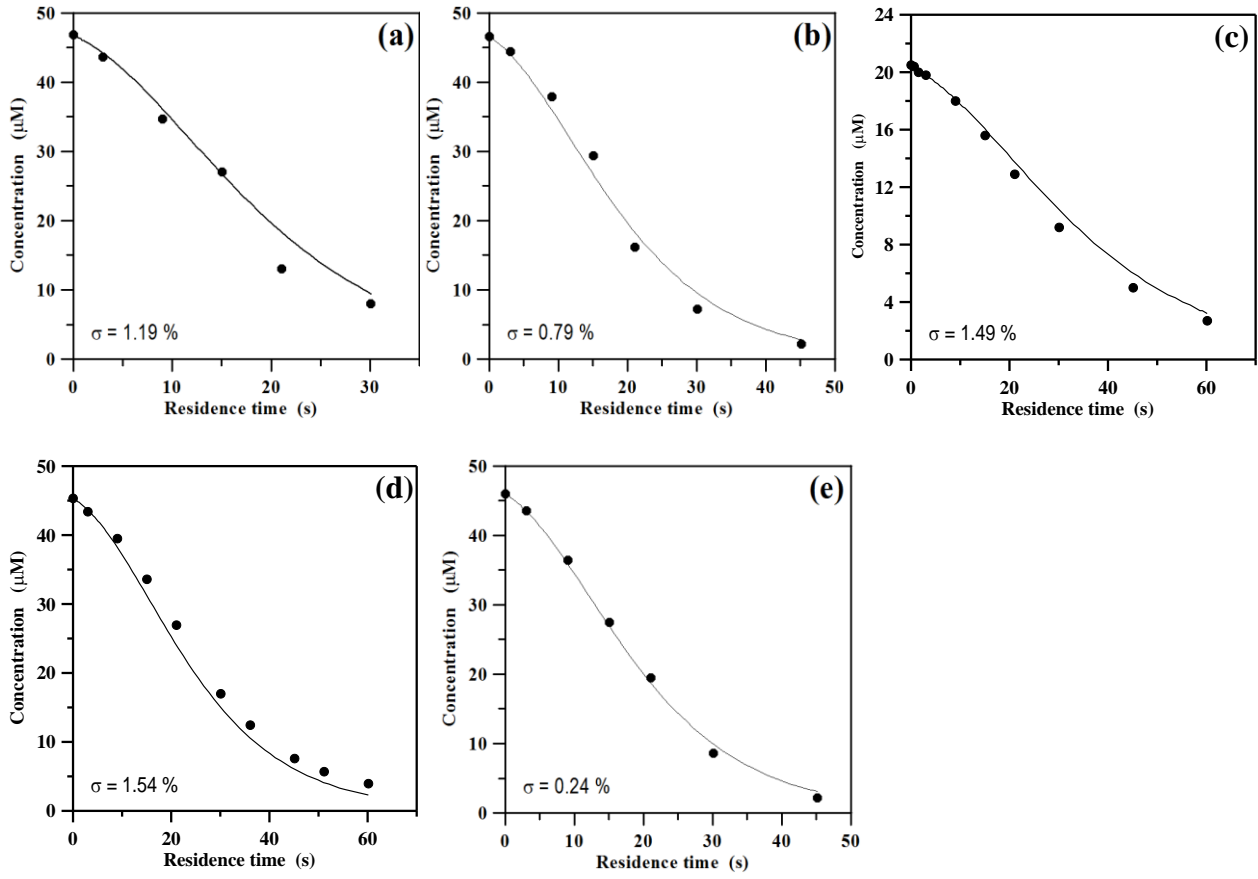


Figure 1

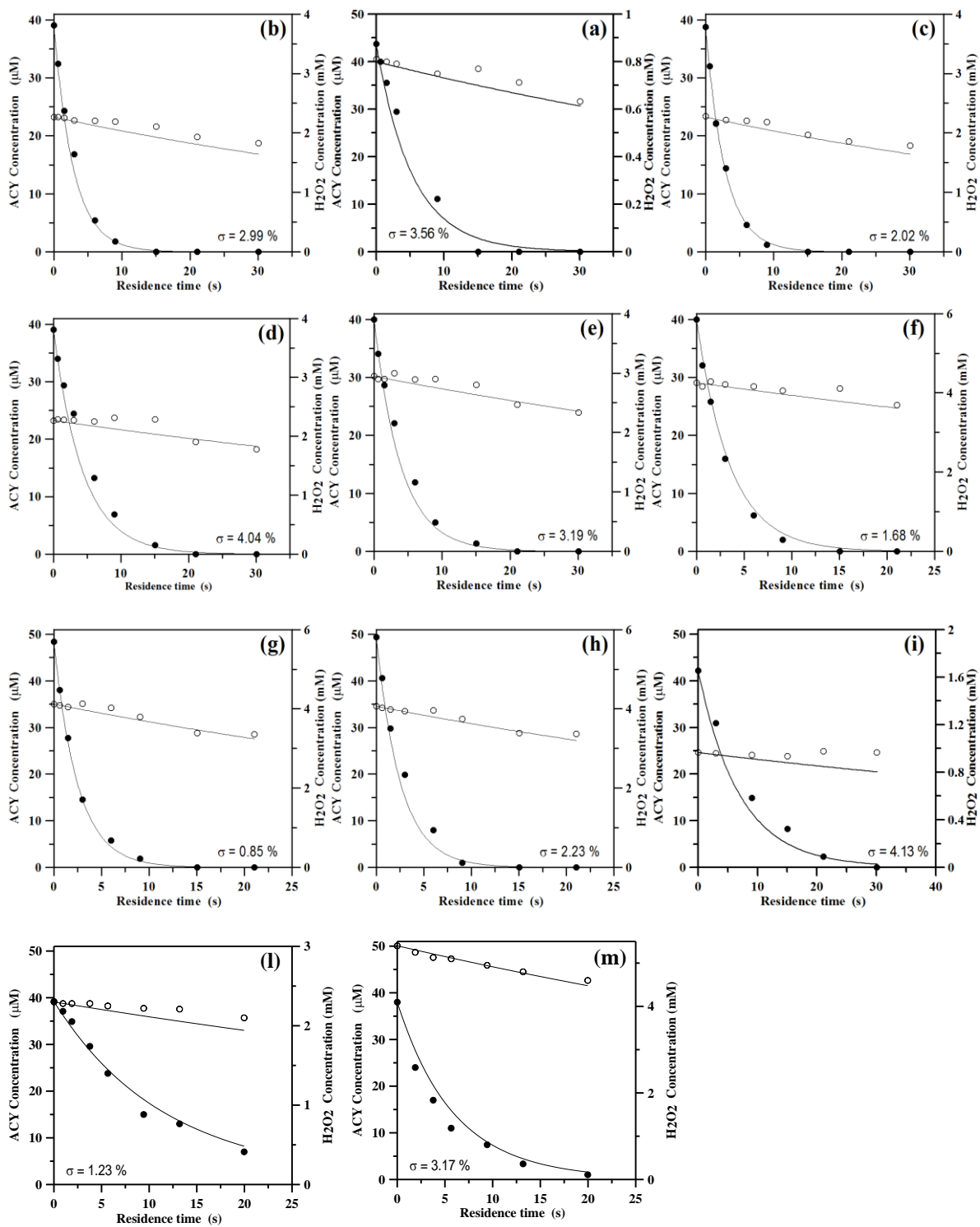


Figure 2

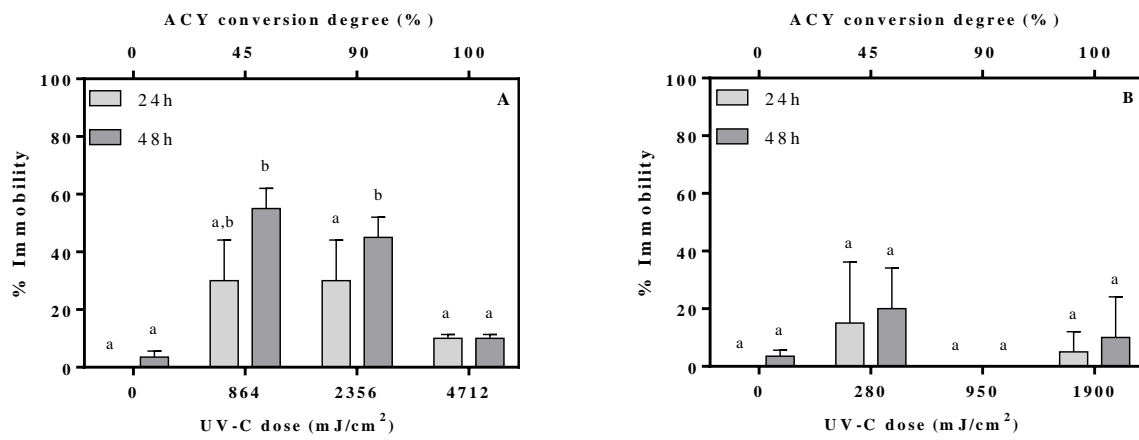


Figure 3



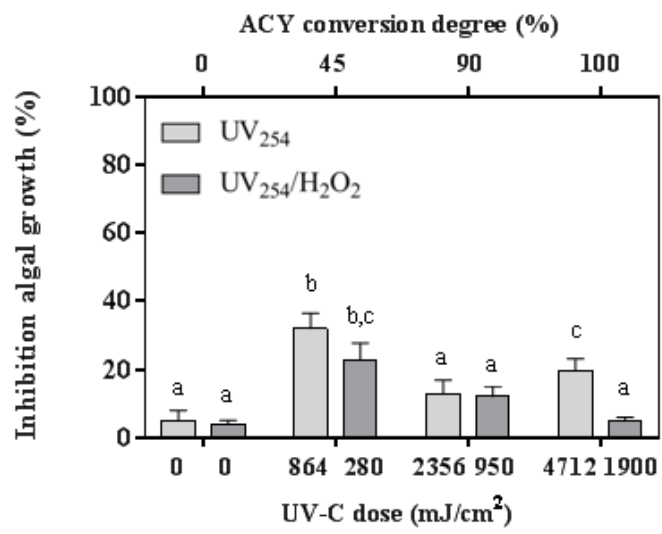


Figure 4

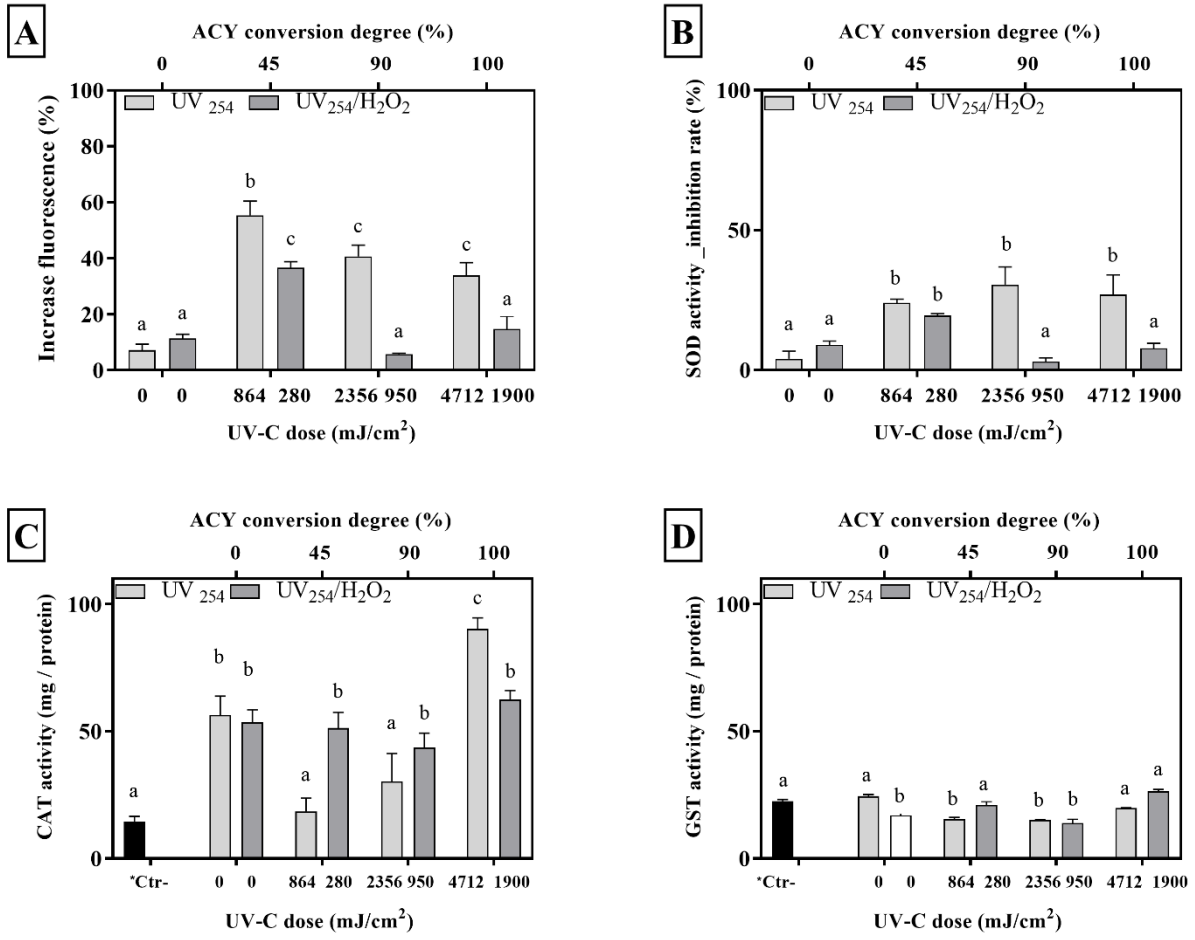


Figure 5

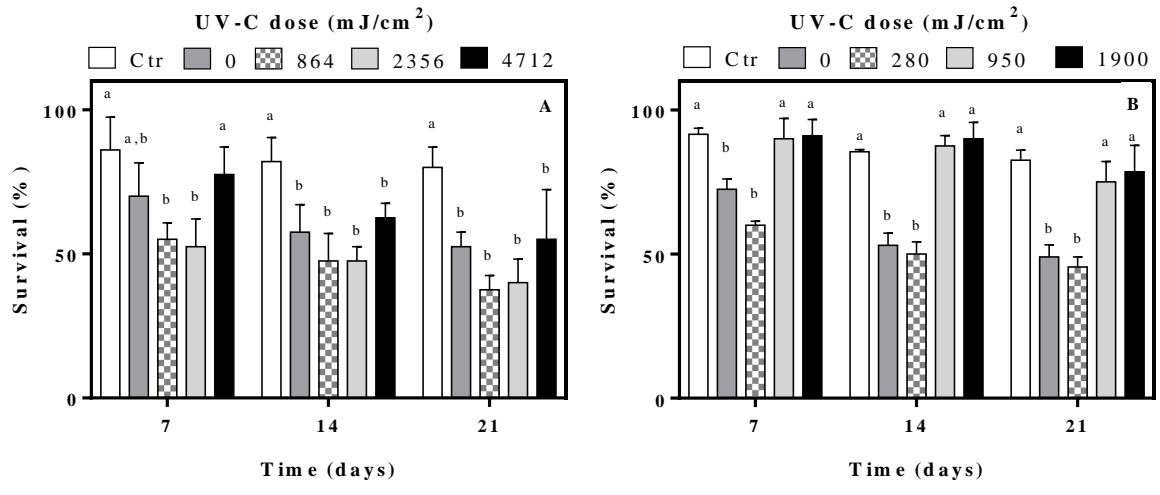


Figure 6

**Figure 1:** Comparison between experimental (circle) and predicted (line) data for UV<sub>254</sub> photolysis of ACY at different pH and power of lamp in the MCF photoreactor.

(a) pH = 6.0 (8.0 W); (b) pH = 4.0 (8.0 W); (c,d) pH = 6.0 (4.5 W); (e) pH = 8.5 (8.0 W).

**Figure 2:** Comparison between experimental (circle) and predicted (line) data for UV<sub>254</sub>/H<sub>2</sub>O<sub>2</sub> photodegradation of ACY (●) and hydrogen peroxide (○) in the MCF photoreactor at different pH, power of lamp and starting H<sub>2</sub>O<sub>2</sub> load. *Optimization mode (a-f), simulation mode (g-m).*

(a): pH = 6.0 (8.0 W, [H<sub>2</sub>O<sub>2</sub>]<sub>0</sub>/[ACY]<sub>0</sub> = 20); (b): pH = 6.0 (8.0 W, [H<sub>2</sub>O<sub>2</sub>]<sub>0</sub>/[ACY]<sub>0</sub> = 50);

(c): pH = 8.0 (8.0 W, [H<sub>2</sub>O<sub>2</sub>]<sub>0</sub>/[ACY]<sub>0</sub> = 50); (d): pH = 6.0 (4.5 W, [H<sub>2</sub>O<sub>2</sub>]<sub>0</sub>/[ACY]<sub>0</sub> = 50);

(e): pH = 6.0 (4.5 W, [H<sub>2</sub>O<sub>2</sub>]<sub>0</sub>/[ACY]<sub>0</sub> = 70); (f): pH = 6.0 (4.5 W, [H<sub>2</sub>O<sub>2</sub>]<sub>0</sub>/[ACY]<sub>0</sub> = 100);

(g): pH = 4.0 (8.0 W, [H<sub>2</sub>O<sub>2</sub>]<sub>0</sub>/[ACY]<sub>0</sub> = 100); (h): pH = 8.2 (8.0 W, [H<sub>2</sub>O<sub>2</sub>]<sub>0</sub>/[ACY]<sub>0</sub> = 100);

(i): pH = 4.0 (4.5 W, [H<sub>2</sub>O<sub>2</sub>]<sub>0</sub>/[ACY]<sub>0</sub> = 20); (l) pH = 6.0 (8.0 W, [H<sub>2</sub>O<sub>2</sub>]<sub>0</sub>/[ACY]<sub>0</sub> = 60);

(m) pH = 6.0 (8.0 W, [H<sub>2</sub>O<sub>2</sub>]<sub>0</sub>/[ACY]<sub>0</sub> = 142).

**Figure 3:** Evolution of acute toxicity with *D. magna* (24 h and 48h) during the UV<sub>254</sub> (A) and UV<sub>254</sub>/H<sub>2</sub>O<sub>2</sub> (B) treatments. Data with different letters (a-b) are significantly different (Tukey's, p<0.05).

**Figure 4:** Toxicity data with *R. subcapitata* (72 h). Data with different letters (a–c) are significantly different (Tukey's, p<0.05).

**Figure 5:** Effects of UV<sub>254</sub> and UV<sub>254</sub>/H<sub>2</sub>O<sub>2</sub> processes on (A) ROS production, (B) SOD, (C) Cat, (D) GST in *Daphnia magna* after 48 h of exposure. For each parameter, mean and standard deviation are shown. Data with different letters (a-d) are significantly different (Tukey's, p<0.05).

\*Ctr- (negative control)

**Figure 6:** Survival curves of *D. magna* during the time of exposure (21 days) for UV<sub>254</sub> (A) and UV<sub>254</sub>/H<sub>2</sub>O<sub>2</sub> (B) treated solutions. Data with different letters (a-b) are significantly different (Tukey's, p<0.05). Dilution: 1:100.

**Table 1:** Occurrence of ACY in WWTP effluents and in surface waters.

**Table 2:** Reaction kinetics mechanism of ACY photooxidation by UV<sub>254</sub>/H<sub>2</sub>O<sub>2</sub> process and mass balance equations. The terms  $f_{H_2O_2}$  and  $f_{ACY}$  indicate the fraction of UV<sub>254</sub> radiation absorbed by hydrogen peroxide and ACY respectively. The TPs concentration was assumed equal to the amount of ACY consumed ( $[ACY]_0 - [ACY]$ ).

$\epsilon_{254}^{H_2O_2}$  and  $\phi_{H_2O_2}$  are the molar absorption coefficient and the quantum yield of photolysis of for hydrogen peroxide at 254 nm respectively.

**Table 3:** First brood and live offspring after 21 days of *D. magna* exposure for different UV<sub>254</sub> doses (with and without hydrogen peroxide).

**Table 4:** Molecular structures of the chemical species identified from the MS spectra of samples submitted to UV<sub>254</sub> and UV<sub>254</sub>/H<sub>2</sub>O<sub>2</sub> photolysis.

<sup>(c)</sup> The structures proposed on the basis of the pseudo-molecular  $[M+H]^+$  ion due to the low intensity of the MS/MS fragmentation signals.